Atmospheric Environment 287 (2022) 119273

Contents lists available at ScienceDirect

Atmospheric Environment

journal homepage: www.elsevier.com/locate/atmosenv

Contributions of domestic sources to $PM_{2.5}$ in South Korea

Naresh Kumar [a,*], Jeremiah Johnson [b], Greg Yarwood [b], Jung-Hun Woo [c], Younha Kim [d], Rokjin J. Park [e], Jaein I. Jeong [e], Suji Kang [f], Sungnam Chun [f], Eladio Knipping [g]

[a] Desert Research Institute, Reno, NV, 89512, USA
[b] Ramboll, Novato, CA, 94945, USA
[c] Konkuk University, Seoul, 05029, South Korea
[d] International Institute for Applied Systems Analysis, Laxenburg, Austria
[e] Seoul National University, Seoul, 08826, South Korea
[f] Korean Electric Power Research Institute, Munji-dong, Daejeon, 3405, South Korea
[g] Electric Power Research Institute, Palo Alto, CA, 94304, USA

HIGHLIGHTS

- A regional air quality model estimated domestic contributions from different sources and regions to PM2.5 in Korea.
- Boundary conditions (includes contributions from China) contributed 30% to 50% towards PM2.5 in major cities in Korea.
- Among the domestic sources, mobile sources contributed the most towards PM2.5 in Korea followed by the industrial sources.
- Our results are qualitatively similar to previous source attribution studies of PM2.5 in Korea.

ARTICLE INFO

Keywords:
Korea air quality
Emissions controls
Particulate matter ($PM_{2.5}$)
Source contributions
CAMx
PSAT

ABSTRACT

We use the CAMx (Comprehensive Air Quality Model with Extensions) chemical transport model (CTM) with 4-km horizontal resolution over the Korean Peninsula to investigate source contributions to $PM_{2.5}$ in Korea from domestic and upwind sources. We modeled 2015 and 2016 to account for meteorological variation with Korean emissions from the Clean Air Policy Supporting System (CAPSS), meteorology from WRF (Weather, Research, and Forecasting) model, and regional boundary concentrations from the GEOS-Chem global CTM. The CAMx particulate source apportionment technology (PSAT) provided $PM_{2.5}$ source contributions from 5 source sectors and 6 geographic regions within Korea, international sources, and boundary concentrations. $PM_{2.5}$ contributions from outside Korea are important with boundary concentrations plus the "other" emissions sector (includes marine shipping, agricultural ammonia, and international emissions from North Korea and Japan within the CAMx domain) contributing 67% of annual average $PM_{2.5}$ in Seoul in 2016 and 71% in 2015. The boundary concentrations contributed between 30% and 50% of $PM_{2.5}$ at different Korean cities with contributions generally lower in 2016 than in 2015. For Korean sources, $PM_{2.5}$ contributions from Electric Generating Unit (EGU) emissions were smaller than contributions from mobile and industrial emissions sources although there is considerable day-to-day variation in contributions. On an annual basis in 2016, the "other" category contributed 25% followed by mobile sources at 23%, industrial sources at 6%, and EGU sources at 3%. For 2015, the contributions were similar. Focusing on March when $PM_{2.5}$ concentrations were higher than other months, the contributions from other, mobile, industrial, and EGUs were 21%, 18%, 4%, and 4%, respectively in 2016. For 2015, contributions from these four categories were 18%, 15%, 3%, and 3%, respectively.

1. Introduction

$PM_{2.5}$ is a key pollutant of health concern in the Republic of Korea (hereafter Korea), especially in cities such as Seoul (Son et al., 2012; Kim et al., 2018; Bae et al., 2019). Although a trend of decreasing $PM_{2.5}$ concentrations has been observed (Kim and Lee, 2018), the

* Corresponding author.
E-mail address: Naresh.Kumar@dri.edu (N. Kumar).

https://doi.org/10.1016/j.atmosenv.2022.119273
Received 27 January 2022; Received in revised form 10 June 2022; Accepted 4 July 2022
Available online 11 July 2022

Fig. 1. Horizontal extent of the WRF (red) and CAMx (blue) 4 km domains. (For interpretation of the references to colour in this figure legend, the reader is referred to the Web version of this article.)

concentrations remain above the national standards (15 μg/m^3 annual and 35 μg/m^3 daily). For example, Kim et al. (2020) examined the hourly and quarterly concentrations of PM_{10} and $PM_{2.5}$ in seven metropolitan areas and Jeju island in Korea from January 2015 to September 2019 and showed that $PM_{2.5}$ levels decreased until 2018 and rebounded in 2019, with concentrations consistently higher in spring and winter. To inform policies to reduce $PM_{2.5}$ concentrations in the country, it is important to fully understand the contribution of different emission sources within Korea under different meteorological conditions. This information can be used to develop effective control strategies to improve air quality. While several apportionment studies have focused on the contribution of international sources (e.g., Kim et al., 2017; Bae et al., 2019; Choi et al., 2019; Bae et al., 2020; Kumar et al., 2021), fewer studies also examined domestic sources of $PM_{2.5}$ pollution (e.g., Choi et al., 2013; Jeong et al., 2017).

A review of Korean source apportionment studies by Ryou et al. (2018) found that motor vehicles, soil dust, and combustion/industry sources were the biggest domestic contributors to PM_{10} and $PM_{2.5}$ in the country. Secondary aerosol (that includes sulfates, nitrates, and secondary organic aerosol (SOA)) contributed more than 35% of $PM_{2.5}$. Many of the previous source apportionment studies for emissions sources in Korea have relied on receptor models. For example, Heo et al. (2009) used positive matrix factorization (PMF) in Seoul and showed that secondary nitrate (21%), secondary sulfate (21%), and gasoline fueled vehicles (17%) were major contributors to $PM_{2.5}$ followed by biomass burning (12%) and diesel emissions (8%).

Choi et al. (2013) analyzed the chemical composition of $PM_{2.5}$ collected at Incheon, Korea every third day from June 2009 to May 2010 and used PMF to identify sources of $PM_{2.5}$. The major source factors were secondary nitrate (25.4%), motor vehicles (23.0%), and secondary sulfate (19.0%) followed by industry (8.5%), biomass burning (6.1%), soil (6.1%), combustion and copper production emissions (6.1%), and sea salt (5.9%). Jeong et al. (2017) used three different receptor models (principal component analysis/absolute principal component score (PCA/APCS), PMF, and chemical mass balance (CMB)) to estimate contributions of various $PM_{2.5}$ emission sources to ambient $PM_{2.5}$ levels during 2013 in Busan, a port city in Korea. They showed that the secondary formation of $PM_{2.5}$ was the dominant (45–60%) contributor to $PM_{2.5}$ levels and that source contribution estimates to $PM_{2.5}$ levels differed significantly among the models indicating their limitations. Oh and Park (2020) analyzed $PM_{2.5}$ concentration data collected from multiple sites in Seoul and estimated regional source profiles using a Bayesian multivariate receptor model. They showed that traffic source affects the entire city quite evenly except for some undeveloped areas and that the industrial sources affect South-Western and North-Eastern regions of Seoul. They also showed that the effect of thermal power plant emissions on $PM_{2.5}$ in 'Mapo' and 'Yangcheon' districts was significant.

While receptor models are useful in identifying source factors contributing to $PM_{2.5}$ in a particular location, they don't identify specific

source categories contributing to concentrations of $PM_{2.5}$ in that location (e.g., a "secondary sulfate" factor that doesn't include information on actual sources). Therefore, chemical transport models (CTMs) are needed to estimate source contributions that take into account secondary chemistry and long-range transport. Several studies using CTMs for Korea have differentiated contributions of international emissions and domestic emissions to $PM_{2.5}$ in Korea. For example, Kim et al. (2017) used a regional air quality model to show that while foreign emissions contributed more than ~60% of $PM_{2.5}$ in Seoul, local contributions were also significant in inland cities. Bae et al. (2019) conducted regional air quality modeling using Community Multiscale Air Quality (CMAQ) model for the east Asia domain for the 2012–2016 period and performed a set of sensitivity simulations to estimate that the annual averaged impact of emissions from China on Seoul $PM_{2.5}$ concentrations ranged from 41% to 44% during the five years. Bae et al. (2020) conducted a modeling study using the CMAQ model from 2010 to 2017 using two different horizontal resolutions (27- and 9- km). They estimated that contributions of emissions from China to annual $PM_{2.5}$ in different provinces in Korea on average for the 8-year period was 58% and 56%, respectively for the 27-km and 9-km resolution. However, the range in Chinese contributions for individual sites was quite wide and therefore they recommend using finer resolutions to better capture the local dynamics and the jurisdictional boundaries.

Here, we report a comprehensive analysis of $PM_{2.5}$ contributions in Korea from 30 emission categories, i.e., 5 inventory sectors in 6 geographic regions, and boundary concentrations for two years (2015 and 2016) using the Comprehensive Air Quality Model with extensions (CAMx) run at 4-km horizontal resolution and with extensive model evaluation. We also evaluated the emissions data used in the model as well as the meteorology used by CAMx for both years.

2. Methods

We used CAMx version 7.0 (Ramboll, 2019) to conduct the source apportionment modeling in Korea. Fig. 1 shows the 4 km horizontal resolution modeling domain which covers Korea and portions of several neighboring countries. The domain is defined on a Lambert Conformal Conic (LCC) projection centered at 36°N, 128°E with true latitudes at 30°N and 40°N. We simulated the 2015 and 2016 calendar years.

Meteorological input data for CAMx were developed using the Weather Forecasting and Research (WRF Version 4.0.1; NCAR, 2018) model nudged by European Center for Medium-Range Weather Forecast (ECMWF) atmospheric analyses. WRF was configured with nested 36, 12 and 4 km grids (Figure S-4 in Supplemental Information (SI)) and the 4 km grids for WRF and CAMx are aligned (Fig. 1), although the WRF grid is slightly larger so that any numerical artifacts near the WRF 4 km nested domain boundary do not influence CAMx. CAMx has 25 layers extending through 20 km with 10 layers in the lowest 1 km and a 20 m deep surface layer. The WRFCAMx preprocessor reformatted WRF output for input to CAMx and diagnosed vertical turbulent exchange coefficients (Kv) that determine vertical mixing of pollutants within CAMx. We adjusted Kv over urban areas to enhance vertical mixing in the lowest 200 m due to heat island and mechanical mixing effects. Additionally, we ensured that vertical mixing occurs below and through convective clouds by raising the planetary boundary layer (PBL) depth to the cloud tops.

Boundary concentrations (BCs) that describe air quality entering the CAMx 4 km grid were provided by simulations that we conducted using the GEOS-Chem global model (Harvard University, 2018) for both 2015 and 2016 (Kumar et al., 2021). Land cover data to characterize surface conditions in CAMx, such as surface roughness, deposition parameters, vegetative distribution, and water/land boundaries, were from the MODIS International Geosphere-Biosphere Programme (MODIS-IGBP) data set available with WRF (Friedl et al., 2010). CAMx used the Carbon Bond version 6 (CB6r4) mechanism for gas-phase chemistry (Emery et al., 2016; Luecken et al., 2019) with the CAMx CF algorithm for $PM_{2.5}$ and PM_{10} chemistry (Ramboll, 2019). More details of the CAMx and WRF configurations are in the SI (Tables S–1).

Table 1
Source categories for source apportionment modeling.

Number	Source Category (sectors included)
1	Natural (biogenic, fire, and sea salt)
2	Electrical generating unit (EGU) point source
3	Industrial point and area sources
4	On-road and off-road mobile sources, including marine ship
5	Other point sources, other area sources, and agricultural fires and ammonia

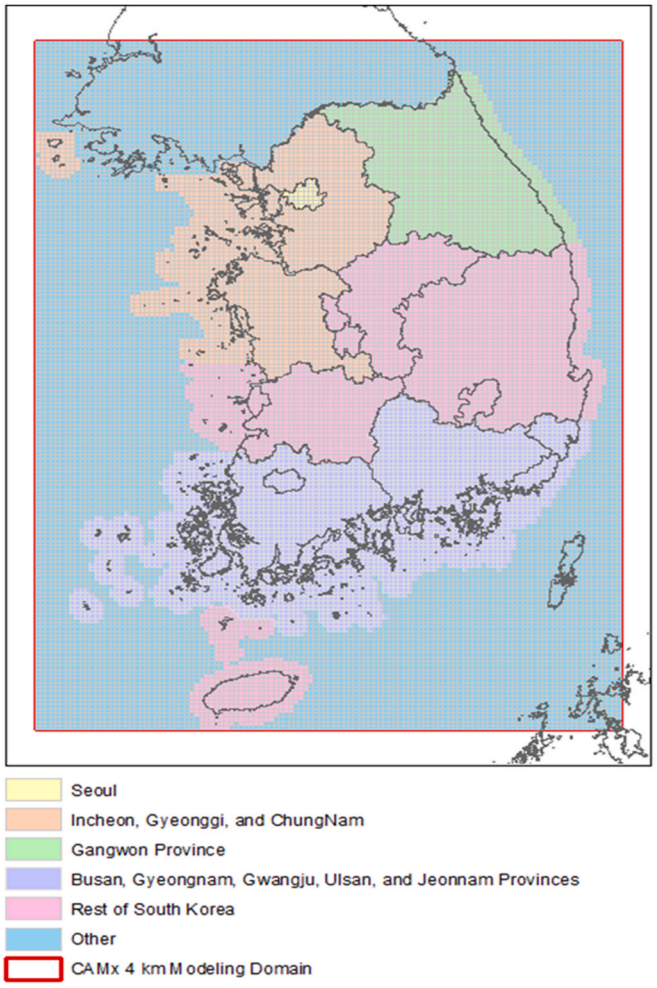

Fig. 2. Geographic regions for PM source apportionment with CAMx PSAT.

To conduct source apportionment, the CAMx model has tagged-species algorithms to explicitly simulate the fate of emissions from specific sources accounting for chemical transformations, transport, and pollutant removal (Ramboll, 2019). We used the Particulate Source Apportionment Technology (PSAT; Yarwood et al., 2007) to apportion both primary and secondary $PM_{2.5}$. We configured PSAT to determine source contributions from 30 emission categories, i.e., 5 emission inventory sectors (Table 1) in 6 geographic regions (Fig. 2), plus the boundary and initial concentrations.

2.1. Emission inventory

The official Korean emissions inventory for air pollutants is called *Clean Air Policy* Supporting *System* (CAPSS) developed by the National Institute of Environmental Research (NIER). CAPSS is a comprehensive

Table 2
2015 and 2016 annual emissions (metric tons per year) in Korea.

Source Category	CO	NO_X	VOC	SO_2	$PM_{2.5}$
Electrical generating unit (EGU) point source	55,138	150,818	7464	91,243	3607
Industrial point and area sources	42,923	228,969	529,149	190,482	41,449
On-road and off-road mobile sources including marine shipping	381,216	673,961	86,456	39,632	22,922
Other point sources, other area sources, and agricultural fires and ammonia	313,497	103,980	387,701	30,934	30,857
Total Anthropogenic	**792,774**	**1,157,728**	**1,010,770**	**352,291**	**98,835**
2015 Biogenic	71,572	4461	619,743	0	0
2015 Wildfire	20,550	1056	5616	127	1705
2015 Sea Salt	0	0	0	0	33,795
2015 Total	**884,896**	**1,163,245**	**1,636,129**	**352,418**	**134,335**
2016 Biogenic	75,413	4881	654,797	0	0
2016 Wildfire	0	0	0	0	0
2016 Sea Salt	0	0	0	0	36,262
2016 Total	**868,187**	**1,162,609**	**1,665,567**	**352,291**	**135,097**

emissions inventory for seven primary pollutants (CO, SO_2, NOx, VOC, NH_3, PM_{10}, and $PM_{2.5}$) that has been used to support multiple local and regional air quality studies (e.g., Kim et al., 2017; Bae et al., 2019; Bae et al., 2020). We used the 2015 CAPSS for both 2015 and 2016 because there was no official inventory available for 2016. More details about the CAPSS emissions are provided in the SI (Tables S–3 and Figures S-1, S-2, and S-3).

We used the latest version of The Sparse Matric Operating Kernel for Emissions (SMOKE, Version 4.5; CMAS, 2018) to develop hourly, gridded, and chemically speciated emissions that are needed by CAMx. During emissions processing, annual emissions inventories were speciated to model species, temporally allocated to hourly emissions, and spatially allocated to grid cells. Biogenic emissions were generated using Model of Emissions of Gases and Aerosols in Nature (MEGAN, Version 2.03), developed at the National Center for Atmospheric Research (NCAR; Sakulyanontvittaya et al., 2008). MEGAN incorporates recent information and has a detailed classification of plant species. We applied MEGAN using hourly meteorology (for example. temperature and solar radiation) from WRF for 2015 and 2016 to generate hourly varying biogenic emissions for the 4 km CAMx modeling domain. Total biogenic VOC emissions over the 4 km domain were calculated to be 824,882 metric tons per year (tpy) for 2015 and 866,278 tpy for 2016. Biogenic emission estimates only for Korea are given in Table 2.

Wildfire emissions are highly episodic and location specific. We used date-specific and geographically resolved estimates of fire emissions from the Fire INventory from NCAR (FINN) that are based on fire detections by satellite (Wiedinmyer et al., 2006, 2011; Wiedinmyer and Friedli, 2007). We modeled fire plume rise as a function of fire area using methods from the Western Regional Air Partnership's (WRAP) Joint Fire Science Program's Deterministic and Empirical Assessment of Smoke's Contribution to Ozone (DEASCO3) project (Mavko and Morris, 2013). Agricultural fire emissions for Korea were included in the CAPSS inventory.

Sea salt emissions contribute to PM in marine and coastal environments. We estimated open-ocean sea salt emissions using a parameterization proposed by Ovadnevaite et al. (2014) which expresses the aerosol flux density function using a combination of multiple lognormally distributed modes for different droplet sizes. We estimated surf-zone (coastal) sea salt emissions with the Gong (2003) parameterization for whitecap fraction (the fraction of the ocean surface covered by whitecaps) and size-dependent droplet production per-unit whitecap area. To obtain hourly-varying sea salt emission estimates we used meteorology (wind speed and sea surface temperature) from the WRF simulations for 2015 and 2016.

Table 2 summarizes the processed emissions of five major pollutants from Korea by source categories used in CAMx source apportionment modeling. Mobile sources are the largest emissions category for NOx followed by industry and EGU point sources. The industrial sources are the largest emitter of SO_2, VOC, and $PM_{2.5}$. The FINN wildfire emissions inventory had no wildfires within Korea in 2016 and for 2015 they were only about 0.5% of total anthropogenic VOC emissions and less than 0.1% of total anthropogenic NOx emissions.

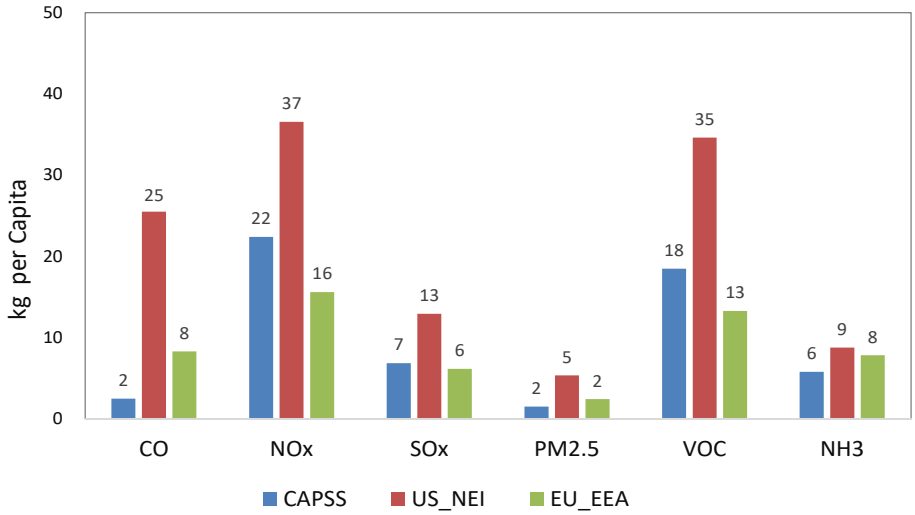

Fig. 3. Per-capita emissions by pollutant (except miscellaneous-other combustion and fugitive dust) (*CO emissions divided by 5).

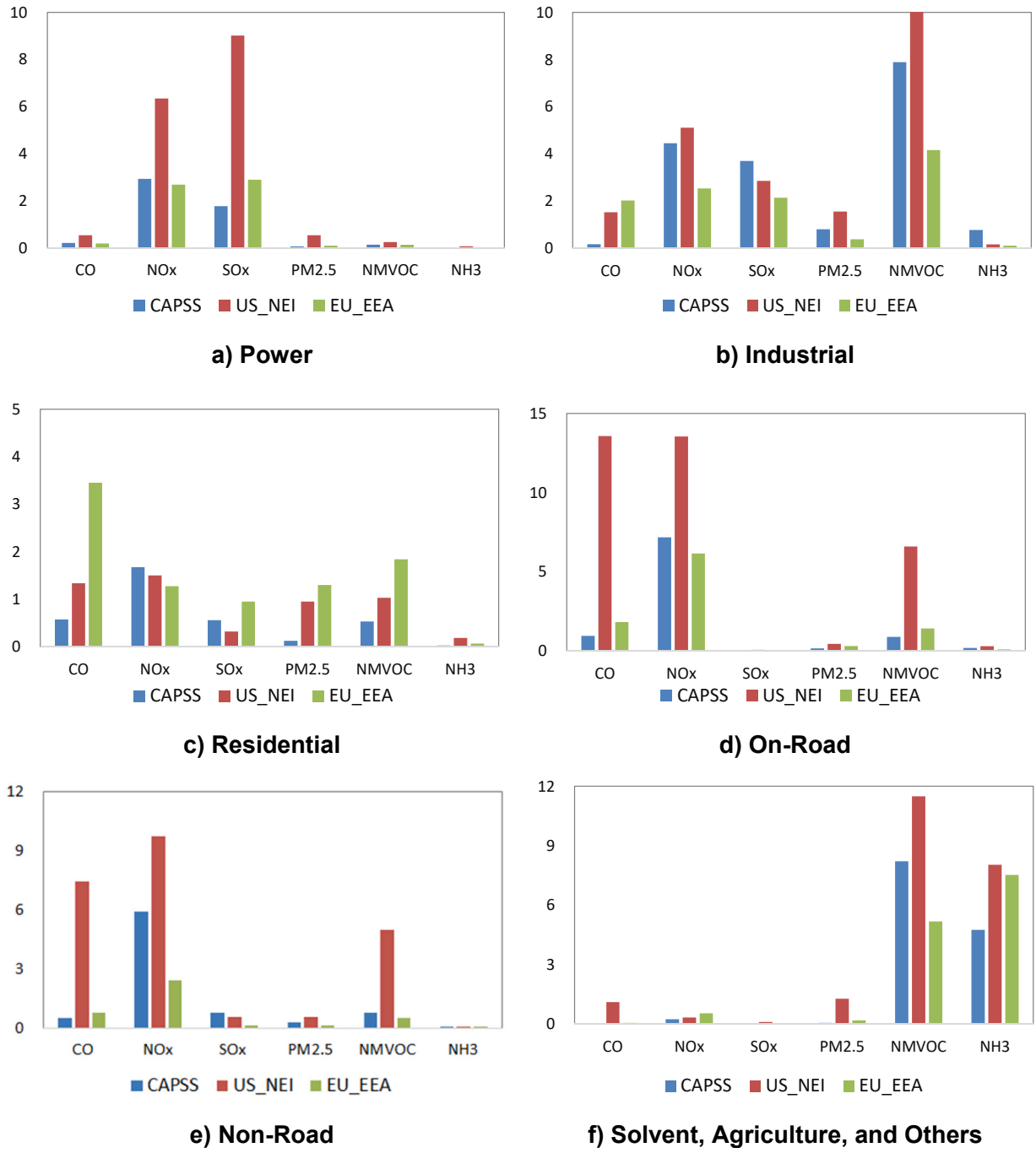

Fig. 4. Per-capita emissions by sector (kg/capita) (except miscellaneous-other combustion and fugitive dust; *CO emissions divided by 5).

3. Results

3.1. Emissions evaluation

Before using the raw emissions from the CAPSS emissions inventory, we evaluated those emissions by comparison with other inventories: the NEI (National Emissions Inventory) of US EPA (Environmental Protection Agency) and EMEP/EEA (European Monitoring and Evaluation Program)/(European Environmental Agency) of EU28 for Years 2014 and 2015, respectively. The NEI is the emissions inventory for the United States compiled by the US EPA. NEI has been estimated every three years, and the latest available inventory available was for 2014 (US EPA,). EMEP/EEA 2015: EMEP/EEA is the emissions inventory of EU28, which is compiled using the CORINAIR system. The version we have used is for 2015.

Fig. 3 shows inter-comparison of per-capita emissions by pollutant. For most pollutants other than CO, US NEI shows a factor of 1.5–2.5 higher per-capita emissions than 2015 CAPSS or EMEP/EEA inventory. For CO, the differences are much higher. The reason that CO emissions are so low in Korea—even compared to EU—is because of the lower industrial and residential sector emissions. Sectoral percentage contribution of CO emissions in CAPSS are similar to US NEI (that is, high mobile sources and biomass-related combustions' contribution), but the amounts are much smaller. This indicates a high possibility of general underestimation of CO emissions in CAPSS across all source sectors in Korea. For the original emissions inventory, US NEI has much higher

per-capita $PM_{2.5}$ emissions compared to Korea and EU because it has much higher biomass burning (e.g., forest fires) and road dust emissions in the inventory. Even though the fires and road dust emissions are also included in the CAPSS inventory, the amounts are much smaller. Unlike in the United States, domestic forest fires and unpaved roads are limited in Korea. Those sectors were omitted in Fig. 3 (for all regions) to make more reasonable comparison among inventories and therefore focus more on fossil-fuel-related similarities.

Fig. 4 shows comparison of per-capita emissions by sector and pollutant. The emissions are higher for the on-road mobile sector, especially in US NEI, which represents higher vehicle use in the United States. For the power and industrial sectors, SOx/NOx and NMVOCs/NOx are the first or second highest emissions in US NEI, which is similar to EEA and CAPSS but with much lower intensity in the latter. The emissions for NH_3 in NEI show higher intensity but with much less difference from CAPSS or EEA emissions. The solvent-agriculture-other sector is significant for NMVOCs and NH_3 emissions.

For the residential sector in Korea, biofuels use (mainly wood combustion) is limited compared to the United States, which is the reason CO and VOCs emissions are relatively low in CAPSS compared to NEI. For VOCs, Simpson et al. (2020) indicated high solvent and mobile contribution in Seoul based on the aircraft measurement–based source apportionment in the KORea-US cooperative Air Quality (KORUS-AQ) aircraft field campaign (NIER and NASA, 2017). In Fig. 4, mobile VOCs in CAPSS are the lowest among three inventories whereas the solvent sector is the highest, which indicates possible underestimation of mobile VOCs and overestimation of the solvent use sector. The agriculture sector in CAPSS includes only NH_3 whereas agricultural burning is also included in NEI. CAPSS shows the lowest per-capita NH_3 emissions, which indicates the country's smaller livestock industry compared to the United States or Europe. Although the Power Sector shows higher emissions for US NEI, there have been significant reductions in those emissions since 2014. Additional evaluation of emissions is provided in the SI.

3.2. Meteorological model evaluation

To evaluate WRF model performance, we used the Surface Data Hourly Global (DS3505) data, which are quality controlled and provide observations at locations determined to be representative of the surrounding geographic area, e.g., measurements at airports. We also investigated whether using meteorological data from the Automatic Weather System (AWS) network operated by the Korea Meteorological Administration (KMA) could improve the WRF evaluation after considering the apparent data representativeness and quality. Performance statistics are compared to established performance benchmarks (Emery et al., 2001; McNally, 2009) to understand how good or poor the results are relative to other model applications. These benchmarks were originally designed for ozone model applications for cities in the eastern and midwestern United States and Texas that were primarily simple (flat) terrain and included simple (stationary high-pressure causing stagnation) meteorological conditions (Emery et al., 2001). More recently, these benchmarks have also been used in meteorological modeling studies that include areas with complex (irregular topography and/or land cover) terrain (McNally, 2009; Environ and Alpine, 2012). Complex conditions can include local scale circulations including mountain-valley winds and land-sea breezes that occur in this study.

The equations for bias and error are shown below, with the equation for the RMSE similar to "Error" except that first the square of the differences between the prediction and observation is taken, and then a square root is taken of the entire quantity.

$$\text{Bias} = \frac{1}{N}\sum_{i=1}^{N}(P_i - O_i)$$

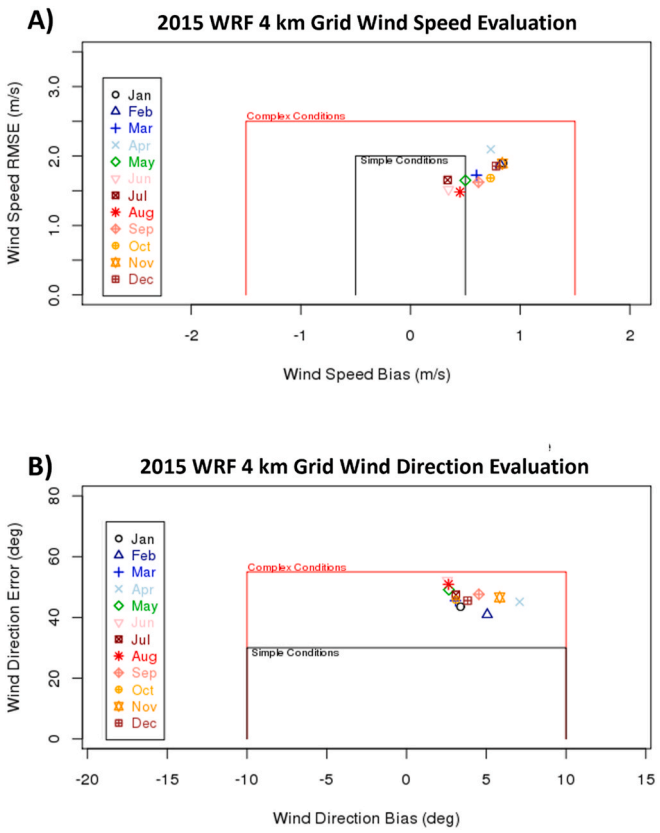

Fig. 5. Monthly WRF bias and error compared to benchmark for complex conditions (red box) for wind speed (top) and wind direction (bottom) at the DS3505 monitors for 2015. (For interpretation of the references to colour in this figure legend, the reader is referred to the Web version of this article.)

$$\text{Error} = \frac{1}{N}\sum_{i=1}^{N}|P_i - O_i|$$

We present the average statistics for each of the four meteorological parameters graphically using the so-called "soccer plot" display. Soccer plots graph monthly average bias versus monthly average error. Along with the results are the simple (plotted in black) and complex benchmark lines (red). It is desirable to have the symbols lay inside the benchmark outline (that is, score a goal in the soccer plot analogy). Using the final WRF model configuration for physics options and domain selection, we completed annual WRF model simulations for the 2015 and 2016 baseline years. Fig. 5 shows soccer plots for the 2015 WRF simulation for wind speed (top) and wind direction (bottom) across all DS3505 monitoring sites within the 4 km WRF domain. Fig. 6 shows similar plots for the 2016 simulation. Soccer plots for temperature and humidity are provided in the SI (Figures S-5 and S-6).

For both simulation years, wind speed and direction exhibit the best performance during the summer months. We find good performance for temperature throughout the duration of the WRF simulations, with several months meeting the simple conditions threshold. We also find good humidity performance for all months in 2015 and 2016. Although humidity shows a consistent negative (dry) bias, it is not large. Only one month (December 2015) is outside of the simple conditions benchmark. Given the complex terrain (that is, coastal, urban, and elevated terrain that generates local-scale circulations) within the modeling domain, these evaluation results demonstrate good WRF performance and suggest that the meteorological inputs are suitable for air quality modeling.

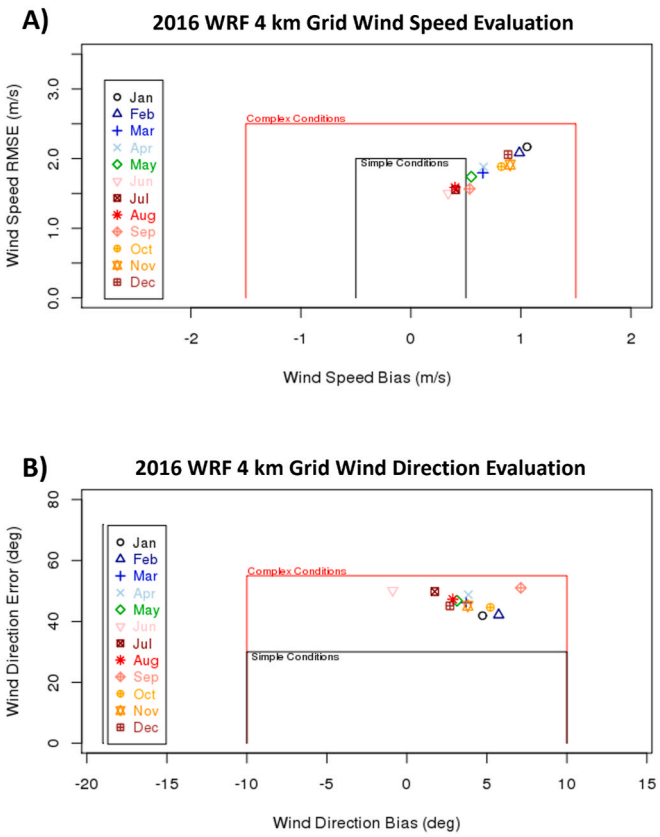

Fig. 6. Monthly WRF bias and error compared to benchmark for complex conditions (red box) for wind speed (top) and wind direction (bottom) at the DS3505 monitors for 2016. (For interpretation of the references to colour in this figure legend, the reader is referred to the Web version of this article.)

3.3. Evaluation of the 2016 CAMx simulation

The data sources used in the CAMx evaluation include the Air Quality Monitoring Station (AQMS) network and six PM supersites in Korea operated by NIER at locations shown in Fig. 7. The AQMS network provides hourly concentrations for CO, NO_2, O_3, $PM_{2.5}$, PM_{10}, and SO_2, which are available to the public (http://www.airkorea.or.kr). The six PM supersites provide daily average measurements for speciated PM components (Korea Ministry of Environment, 2018).

Performance statistics are compared to performance benchmarks (Goals and Criteria) proposed by Emery et al. (2017) for ozone and $PM_{2.5}$. "Goals" indicate statistical values that should be viewed as the best a model can be expected to achieve. "Criteria" indicate statistical values that should be viewed as what a majority of models have achieved.

The model performance evaluation for the initial model run for 2016 revealed that some pollutants had high positive bias (or biased high) and others had high negative bias (or biased low). SO_2 was biased high in restricted locations near major sources. Ozone was biased high in most areas, suggesting that regional background may be overestimated. Isoprene concentrations were high in forested areas. $PM_{2.5}$ nitrate was biased high at all supersite locations (rural and urban). $PM_{2.5}$ ammonium was biased high at all supersite locations. VOC was biased low in Seoul and surrounding areas. CO was biased low in all areas. $PM_{2.5}$ OA (organic aerosol) was biased low at supersite locations but high in some unmonitored locations near major sources.

We investigated potential causes of these biases with a series of diagnostic simulations and based on those simulations, made several adjustments to CAMx input data that are reasonable on a technical basis and also improve agreement with observations. We reduced GEOS-Chem boundary conditions (BCs) for particulate nitrate (PNO_3), HNO_3, particulate ammonium (PNH_4), and NH_3 by half because those were too high based on comparison against aircraft data (NIER and NASA, 2017). We increased GEOS-Chem BCs for particulate sulfate (PSO_4) and SO_2 by 30% to account for underpredictions in the model (Kumar et al., 2021). Finally, we reduced the biogenic isoprene emissions factor by half, and further reduced isoprene emissions in urban areas by accounting for built areas that are inadequately differentiated

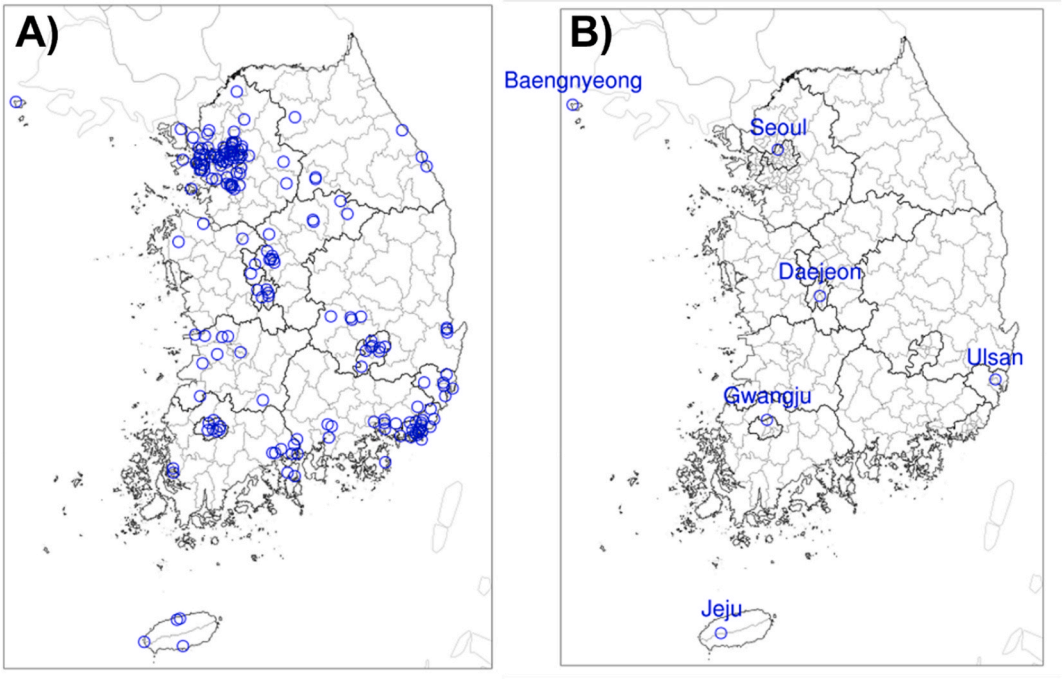

Fig. 7. The NIER AQMS network (left) and $PM_{2.5}$ supersites (right).

Table 3
CAMx model performance statistical summary for 2016 simulation. Statistics for ozone, NO_2, and SO_2 are averaged across all NIER stations. Units for $PM_{2.5}$ are μg/m^3 and ppb for ozone, NO_2, and SO_2.

	# Obs	Mean Observed	Mean Predicted	Bias	r	NMB (%)	NME (%)
$PM_{2.5}$ (NIER)	46,292	26.2	20.0	−6.2	0.471	−23.5	41.3
$PM_{2.5}$ Seoul	348	27.4	19.7	−7.7	0.606	−28.4	38.5
$PM_{2.5}$ Daejeon	352	29.7	18.0	−11.7	0.567	−38.9	45.4
$PM_{2.5}$ Gwangju	345	25.5	16.4	−9.1	0.590	−35.2	42.4
$PM_{2.5}$ Ulsan	358	22.2	15.4	−6.8	0.637	−30.3	40.5
$PM_{2.5}$ Jeju	318	13.9	9.6	−4.3	0.594	−30.5	51.8
$PM_{2.5}$ Baengnyeong	348	21.7	12.6	−9.1	0.635	−40.8	47.8
Ozone MDA8	45,918	41.0	48.3	7.3	0.707	17.6	30.4
Ozone MDA1	46,437	48.5	55.1	6.6	0.714	13.3	27.4
NO_2 MDA1	47,081	40.3	48.7	8.4	0.478	20.9	43.1
NO_2 24-hr	47,081	23.2	26.1	2.9	0.581	12.7	40.9
SO_2 MDA1	46,011	8.2	11.3	3.1	0.421	37.4	79.1
SO_2 24-hr	46,011	4.6	5.2	0.7	0.423	14.5	65.5

Table 4
Bias in CAMx model predictions by season for the 2016 simulation. Units for $PM_{2.5}$ are μg/m^3 and ppb for ozone, NO_2, and SO_2. DJF refers to December, January, and February and so on for MAM, JJA, and SON.

	Bias				
	Annual	DJF	MAM	JJA	SON
$PM_{2.5}$ (NIER)	−6.2	−11.9	−6.8	−2.3	−3.9
$PM_{2.5}$ Seoul	−7.7	−14.0	−10.1	−1.7	−4.7
$PM_{2.5}$ Daejeon	−11.7	−20.4	−11.5	−6.4	−8.3
$PM_{2.5}$ Gwangju	−9.1	−15.2	−8.2	−5.4	−7.6
$PM_{2.5}$ Ulsan	−6.8	−10.6	−7.4	−3.5	−5.4
$PM_{2.5}$ Jeju	−4.3	−10.9	−3.2	0.3	−3.6
$PM_{2.5}$ Baengnyeong	−9.1	−12.3	−9.0	−6.0	−9.0
Ozone MDA8	7.3	7.3	−0.8	13.5	9.5
Ozone MDA1	6.6	6.7	−2.5	12.9	9.0
NO_2 MDA1	8.4	−3.6	4.0	21.9	11.5
NO_2 24-hr	2.9	−3.6	0.4	9.7	5.4
SO_2 MDA1	3.1	2.5	2.9	2.9	4.7
SO_2 24-hr	0.7	0.2	0.7	0.7	1.3

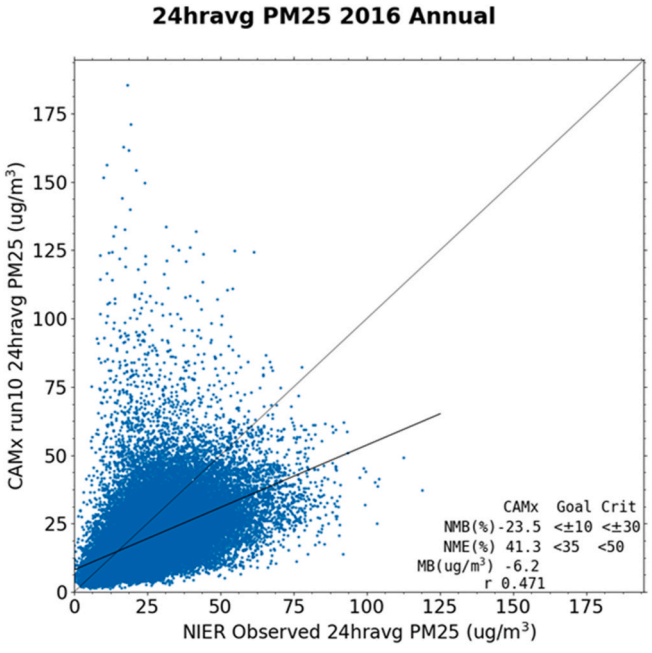

Fig. 8. Scatter plot of observed vs. CAMx 2016 Run10 24-h average $PM_{2.5}$ concentrations at all NIER monitoring sites.

Fig. 9. Map of Seoul showing locations of KIST sampling site and Olympic Park.

by the MEGAN landcover data. Measurements during KORUS-AQ showed isoprene concentrations to be ~0.5 ppb on average (Sullivan et al., 2019), whereas our initial simulations were showing much higher concentrations. Adjusting isoprene emissions brought isoprene concentrations to be mostly below 0.5 ppb.

Table 3 provides a summary of model performance statistics for the final simulation based on the various adjustments. The statistics show $PM_{2.5}$ underestimations at each of the six supersites (NMB ranges from −40.8% at Bangnyeong to −23.4% at Seoul) as well as the average of all NIER sites (NMB: -23.5%). Bae et al. (2020) also found bias toward underpredicting $PM_{2.5}$ at six supersites with average NMB of −19.1% for eight years of modeling. Statistics for ozone, NO_2, and SO_2 all show overestimations.

Table 4 provides bias statistics by season to see how the model bias may vary from one season to another for different species. For PM2.5, the bias is generally the highest in winter (December, January, and February) and the lowest in summer (June, July, and August) seasons with the spring (March, April, and May) numbers similar to the annual values. For ozone and NO2, the highest bias occurs in the spring while the lowest is in spring. Overall, the model underestimates PM2.5 as we saw in the annual statistics, but the model performance is within the criteria based on Emery et al. (2017) recommendations.

Fig. 8 shows a scatter plot of daily averaged $PM_{2.5}$ concentrations (observed vs. CAMx) across all NIER sites in 2016. The NMB and NME statistics are well within the criteria and close to the goal benchmarks.

Table 5
Speciated PM_1 component observations (left table) and CAMx (right) $PM_{2.5}$ components for April 14–June 15, 2016 at the KIST sampling site.

KORUS-AQ KIST Measurements (Kim et al., 2018)	Average (μg/m3)	Fraction of PM_1 (%)
Organic Aerosol	9.76	44%
Nitrate	3.78	17%
Sulfate	4.40	20%
Ammonium	2.56	12%
Chloride	0.04	0%
BC	1.52	7%
Total PM_1	22.10	100%

CAMx Model	Average (μg/m3)	Fraction of $PM_{2.5}$ (%)
Organic Aerosol	4.14	19%
Nitrate	5.21	24%
Sulfate	4.13	19%
Ammonium	2.97	14%
Chloride	0.02	0%
BC	1.33	6%
Other $PM_{2.5}$	3.92	18%
Total $PM_{2.5}$	21.72	100%

These statistics suggest good $PM_{2.5}$ model performance. During the KORUS-AQ campaign, a fixed sampling site at the campus of the Korean Institute of Science and Technology (KIST; see Fig. 9) measured speciated PM_1 components as well as precursors to both ozone and PM (Kim et al., 2018). We used these measurements to assess CAMx model performance for individual $PM_{2.5}$ species in Seoul. Table 5 shows the speciated PM_1 component observations at the KIST site compared against the CAMx $PM_{2.5}$ component concentrations for the KORUS-AQ period (April 14 to June 15, 2016). While sulfate, ammonium, and BC compare reasonably well, model overpredicts nitrate and significantly underpredicts organic aerosol. "Other $PM_{2.5}$" in the model refers to crustal matter.

Fig. 10 shows the model performance for 24-h averaged Nitrate (NO3), Ammonium (NH4), and Sulfate (SO4) at three of the supersites: Seoul, Daejeon, and Baengnyeong. Although there is lot of variability in model predictions against the observed values, the overall mean bias is small. The model is within the criteria metrics generally used for speciated PM2.5 except for Nitrate at Baengnyeong where the NMB is slightly above the criteria value. Also, for Ammonium and Sulfate, the NME is slightly above the criteria values at Seoul and Daejeon. Overall, the model performance for speciated PM2.5 is similar to what is seen for typical modeling studies.

3.4. Evaluation of 2015 CAMx simulation

Here we describe the CAMx model performance evaluation for the 2015 baseline year using the same configuration as for 2016. Overall, we find that 2015 performance is very similar to 2016 performance. Table 6 provides a summary of model performance statistics for the CAMx 2015 simulation. The statistics show $PM_{2.5}$ underestimations at each of the six supersites (NMB ranges from −40.1% at Daejeon to −18.9% at Seoul) as well as at the average of all NIER sites (NMB: -15.2%). Similar to 2016, statistics for ozone, NO_2, and SO_2 all show overestimations.

Fig. 11 shows a scatter plot of daily averaged $PM_{2.5}$ concentrations (observed vs. CAMx) across all NIER sites in 2015. The NMB and NME statistics are well within the criteria and close to the goal benchmarks. These statistics suggest reasonably good $PM_{2.5}$ model performance.

3.5. Contribution from sources and source regions within Korea

3.5.1. Contributions for 2016

Fig. 12 shows annual average $PM_{2.5}$ contributions by emissions source category for the six supersites. The largest contribution for each site, labelled *Boundary*, comes from outside the CAMx domain and is determined by the CAMx BCs obtained from GEOS-Chem. The largest boundary contributions are at Jeju (69.1%) and Baengnyeong (82.4%), the two sites closest to the edge of the CAMx domain. The next largest contribution is Other, which includes marine shipping, agricultural ammonia, and international emissions from North Korea and Japan that are within the CAMx domain. EGU contributions are relatively small, ranging from 1.2% (Baengnyeong) to 4.4% (Gwangju) of total $PM_{2.5}$.

Fig. 13 presents the same pie charts as in Fig. 12 but shows the average of the top 10 *p.m.2.5* days in 2016 instead of the annual average to see how the contribution might vary on most polluted days. The boundary contribution decreases for all sites, but Jeju and Gwangju in Fig. 13 compared to what is seen in the annual pie charts in Fig. 12. At these four sites, the non-boundary contributions are larger on the top 10 days, but the composition among these sources varies. At each of the four sites, the EGU contribution is higher on the top 10 days. However, the maximum EGU contribution (Daejeon: 6.2%) is still smaller compared to other source categories (Other: 25.1%; Mobile: 21.7%; Industrial: 11.2%).

Fig. 14 presents the same pie charts as in Fig. 12 but shows the March 2016 monthly average instead of the annual average, as March is the month when the *PM2.5* concentrations are the highest. The boundary contribution increases at all sites in Fig. 14 compared to the annual pie charts shown in Fig. 12.

In Fig. 15, we present box plots showing the distribution of 24-h average $PM_{2.5}$ EGU contributions by emissions source region at the Seoul (top), Daejeon (middle), and Gwangju (bottom) supersites. The dots show contributions for different days, the box shows where the 50% of the contributions lie with the line in the box indicating the median contribution, and the thick lines show lower and upper extremes (values outside of those extremes are considered outliers). Plots for other cities are shown in the SI (Figures S-7 and S-8). The boundary contribution box plot is shown on a separate axis because the values are much larger. The box plots show that the largest daily $PM_{2.5}$ contributions from EGUs at each site come from the Incheon/Gyeonggi/ChungNam region. In Seoul, EGU contributions do not exceed 1.0 $\mu g/m^3$ from any other region.

It is also insightful to examine spatial patterns of contributions from different source categories, so we have included that in Figure S-11 for the annual contribution to PM2.5 from six source categories.

3.5.2. Contributions for 2015

Fig. 16 shows 2015 annual average $PM_{2.5}$ contributions by emissions source category for the six supersites. As with the 2016 results, the largest contribution at each site comes from the CAMx BCs. The largest boundary contributions are at Jeju (71.3%) and Baengnyeong (89.5%), the two sites closest to the edge of the CAMx domain. The next largest contribution is Other, which includes marine shipping, agricultural ammonia, and international emissions from North Korea and Japan that are within the CAMx domain. EGU contributions are relatively small (and very similar to 2016), ranging from 1.1% (Baengnyeong) to 4.1% (Gwangju) of total $PM_{2.5}$.

Fig. 17 presents the same pie charts as in Fig. 16 but shows the average of the top 10 days in 2016 instead of the annual average. For all sites except Jeju, the boundary contribution changes by less than 5% compared to the annual averages. At all six sites, the EGU contribution is slightly higher on the top 10 days (maximum at Gwangju: 4.5%) compared to the annual averages (Gwangju: 4.1%).

Fig. 18 presents the same pie charts as in Fig. 16 but shows the March 2015 monthly average instead of the annual average. The boundary contribution increases at all sites in Fig. 18 compared to the annual pie charts shown in Fig. 16. Although the non-boundary contributions are larger for March compared to the annual averages, the EGU contributions are higher in March for all sites except Baengnyeong.

In Fig. 19, we present box plots showing the distribution of 24-h average $PM_{2.5}$ EGU contributions by emissions source region at the Seoul (top), Daejeon (middle), and Gwangju (bottom) supersites, and similar box plots are shown for Ulsan, Jeju, and Baengnyeong in the SI. (Figures S-9 and S-10). The boundary contribution box plot is shown on

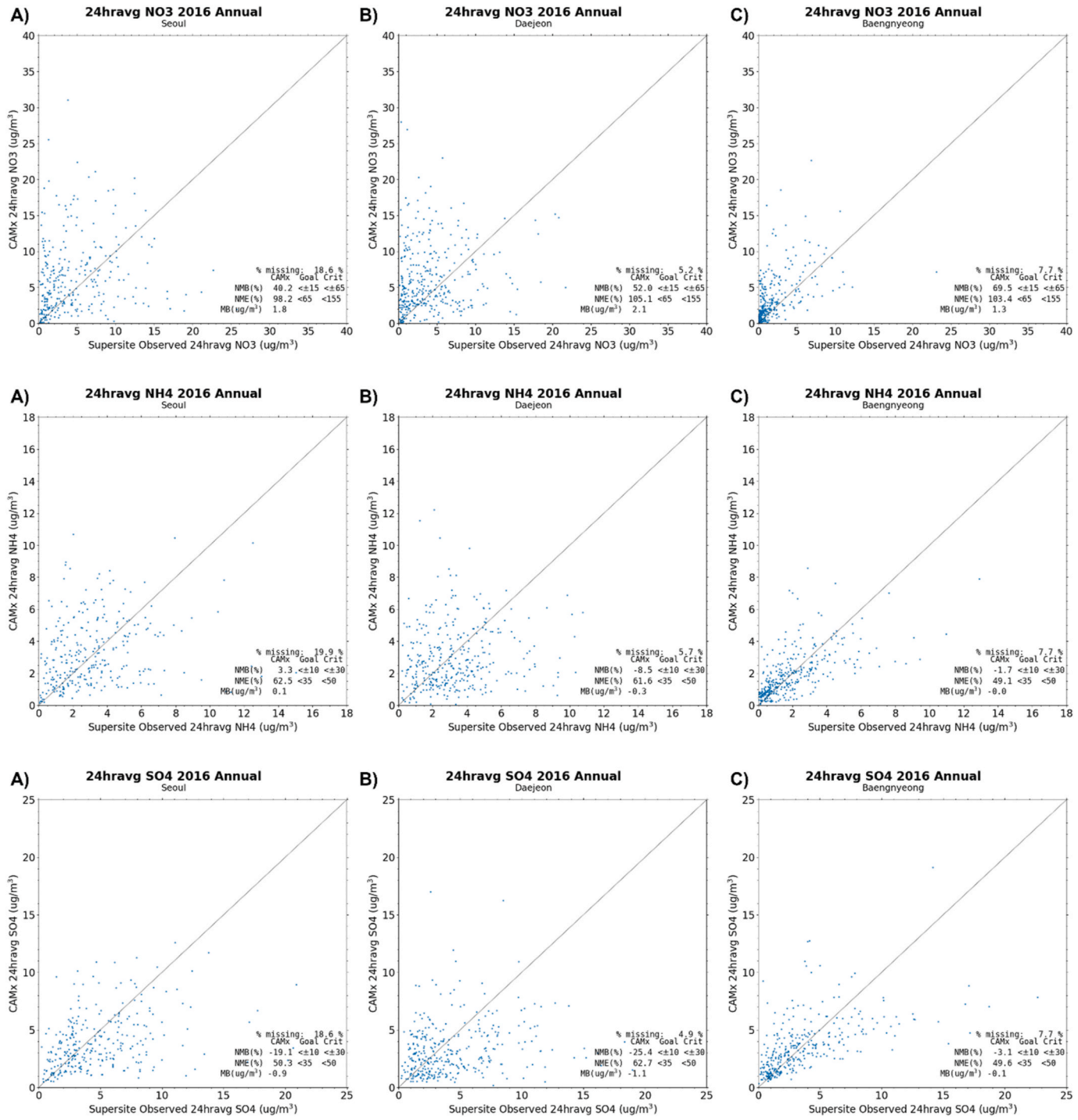

Fig. 10. Scatter plot of observed vs. CAMx 2016 Run10 24-h average Nitrate (top), Ammonium (middle), and Sulfate (bottom) concentrations at Seoul (A), Daejeon (B), and Baengnyeong (C).

a separate axis because the values are much larger. The box plots show that the largest daily $PM_{2.5}$ contributions from EGUs at each site except Jeju and Ulsan come from the Incheon/Gyeonggi/ChungNam region. In Seoul, EGU contributions do not exceed 1.0 μg/m^3 from any other region except for two days. We find the largest EGU contributions at Gwangju, where the annual maximum contribution from the Incheon/Gyeonggi/ChungNam region is 6.9 μg/m^3 and 3.7 μg/m^3 from the Southern Provinces.

Figure S-12 for the spatial distribution of annual contribution to PM2.5 from six source categories.

3.5.3. *Differences between contributions for 2015 and 2016*

In Table 7, we present 2015 and 2016 annual average $PM_{2.5}$ contributions by emissions source region at selected cities near EGU sources. Table 8 presents a similar comparison showing the 2015 and 2016 annual average $PM_{2.5}$ contributions by emissions source category. Overall, results are similar between 2015 and 2016. EGU contributions are relatively small (largest contributions are only 7% of total $PM_{2.5}$ at Boryeong and Taean) and nearly identical between 2015 and 2016 (maximum difference is 0.1 μg/m^3).

Table 6
CAMx model performance statistical summary for 2015 simulation. Statistics for ozone, NO_2, and SO_2 are averaged across all NIER stations.

	# Obs	Mean Observed	Mean Predicted	Bias	r	NMB (%)	NME (%)
$PM_{2.5}$ (NIER)	35,871	25.3	21.3	−4.0	0.585	−15.2	36.4
$PM_{2.5}$ Seoul	362	28.0	22.6	−5.3	0.697	−18.9	33.4
$PM_{2.5}$ Daejeon	331	35.8	21.5	−14.2	0.670	−40.1	44.0
$PM_{2.5}$ Gwangju	358	28.2	20.0	−8.2	0.687	−28.7	38.4
$PM_{2.5}$ Ulsan	360	22.6	17.2	−5.4	0.713	−23.3	34.1
$PM_{2.5}$ Jeju	358	16.1	12.0	−4.1	0.509	−25.5	48.7
$PM_{2.5}$ Baengnyeong	352	23.8	14.9	−8.9	0.619	−36.9	44.8
Ozone (MDA8)	36,526	40.4	48.1	7.7	0.705	18.7	30.7
Ozone (MDA1)	36,916	47.9	54.5	6.7	0.706	13.7	27.7
NO_2 (MDA1)	36,849	40.7	48.8	8.1	0.478	19.9	42.5
NO_2 (24-hr)	36,849	23.5	26.4	2.9	0.612	12.5	40.2
SO_2 (MDA1)	35,816	8.9	11.7	2.9	0.470	32.4	71.9
SO_2 (24-hr)	35,816	5.1	5.5	0.4	0.452	8.5	58.5

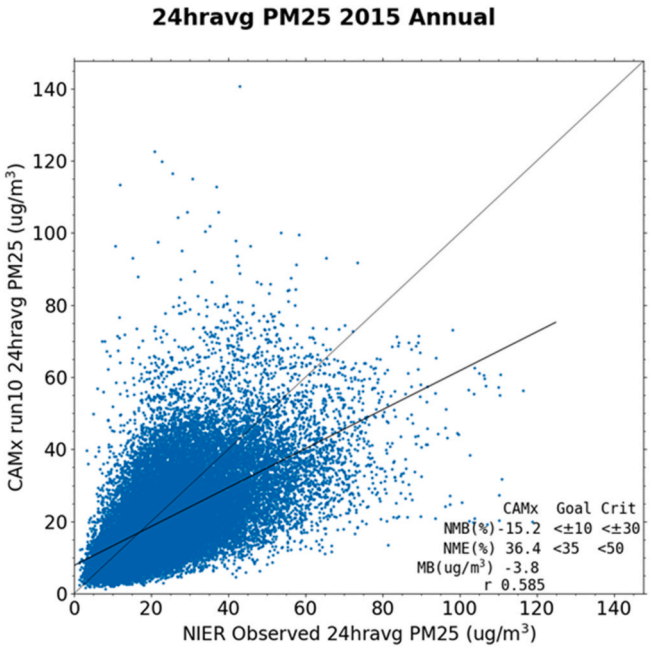

Fig. 11. Scatter plot of observed vs. CAMx 2015 24-h average $PM_{2.5}$ concentrations at all NIER monitoring sites.

4. Discussion

We conducted annual simulations for 2015 and 2016 using CAMx to estimate contributions to $PM_{2.5}$ in Korea from different sources and source regions within Korea. Emissions inventory, the WRF model, and the CAMx model were evaluated extensively before conducting the source apportionment modeling using CAMx.

The CAPSS emission inventory was used for the study, as it is the official emissions inventory for Korea. We compared the CAPSS inventory to the US NEI and EMEP EI to understand limitations of the emissions used in the modeling. For the regional emissions inventories, US NEI has much higher per-capita $PM_{2.5}$ emissions compared to Korea and EU because it has much higher biomass burning (fire) and road dust emissions in the inventory. Without those sectors, 2015 CAPSS showed reasonable per-capita emissions agreements to EMEP EI and US NEI. For most pollutants other than CO, US NEI showed 1.5–2.5 higher per-capita emissions than 2015 CAPSS and EMEP EI, which are in a reasonable range considering socio-economic and geographic differences among the countries/regions. CO emissions comparison, however, indicated general underestimation of CO emissions in CAPSS across all the source sectors in Korea. This, however, should not have affected CAMx results much due to the low chemical reactivity of CO. For VOCs, the solvent emissions were relatively high, and on-road mobile emissions were low in CAPSS, compared to the other two inventories. High solvent use seems reasonable based on the aircraft-based source apportionment in the KORUS-AQ field campaign. Lower VOCs from the on-road mobile sector are indicated, at least in part, due to the higher diesel fleet mix in Korea. For the residential sector in CAPSS, biofuel use is limited compared to NEI, which is the reason CO and VOCs emissions in this sector are low in Korea. The CAPSS showed the lowest per-capita NH_3, which indicates Korea's smaller livestock industry compared to the United States or Europe. Overall, we conclude that the emission inventory data sets selected were reasonably good, even with some limitations, to be used for the air quality modeling. CO emissions across all the sectors and NMVOCs from the mobile and solvent source sectors in the CAPSS inventory should to be improved in the long run.

Evaluation of the CAMx modeling indicated that $PM_{2.5}$ model performance met the benchmark criteria for both 2015 and 2016. There was also good performance for SO_4 and NH_4 while NO_3 was biased high and OA was biased low, which requires further investigation. Overall, model performance between 2015 and 2016 was quite similar. As with 2016, 2015 p.m.$_{2.5}$ concentrations were underestimated at most locations, but the discrepancies from observed values were not large. Although the model evaluation met the benchmark criteria for both years, there are important caveats that must be kept in mind when interpreting the source contribution analysis conducted using the model. There are uncertainties in model inputs (emissions and meteorology) and physical and chemical parameterizations in the model that can influence the results, so there is always some uncertainty around source contribution estimates obtained using models.

Our analysis of the source contribution analysis using CAMx estimated that the boundary contribution combined with the "Other" sector (including marine shipping, agricultural ammonia, and international emissions from North Korea and Japan within the CAMx domain) together contribute 67% of the annual average $PM_{2.5}$ concentration in Seoul in 2016 and 71% in 2015. The boundary conditions were estimated to contribute between 30% and 50% of $PM_{2.5}$ at different cities (e.g., Seoul, Daejeon, Gwangju, etc.) with 2016 contributions lower than 2015 on average. $PM_{2.5}$ contributions from EGU emissions were estimated to be small in comparison to contributions from mobile and industrial emissions sources. The largest daily $PM_{2.5}$ contributions from EGUs at each site come from the Incheon/Gyeonggi/ChungNam region both in 2016 and 2015. In general, there is a lot of variability in contributions from different sources and regions. Among Korean sources, mobile and "Other" were the most important.

Since Seoul is the most populated city in Korea, we provide below specific results for Seoul from the $PM_{2.5}$ contribution analysis using CAMx.

On an annual basis, the "Other" category contributed 25% followed by mobile sources at 23% and industrial sources at 6%. The contribution from EGU was estimated at 3%. Focusing on the top 10 p.m.$_{2.5}$ days, the contributions from other, mobile, industrial, and EGUs were 21%, 27%,

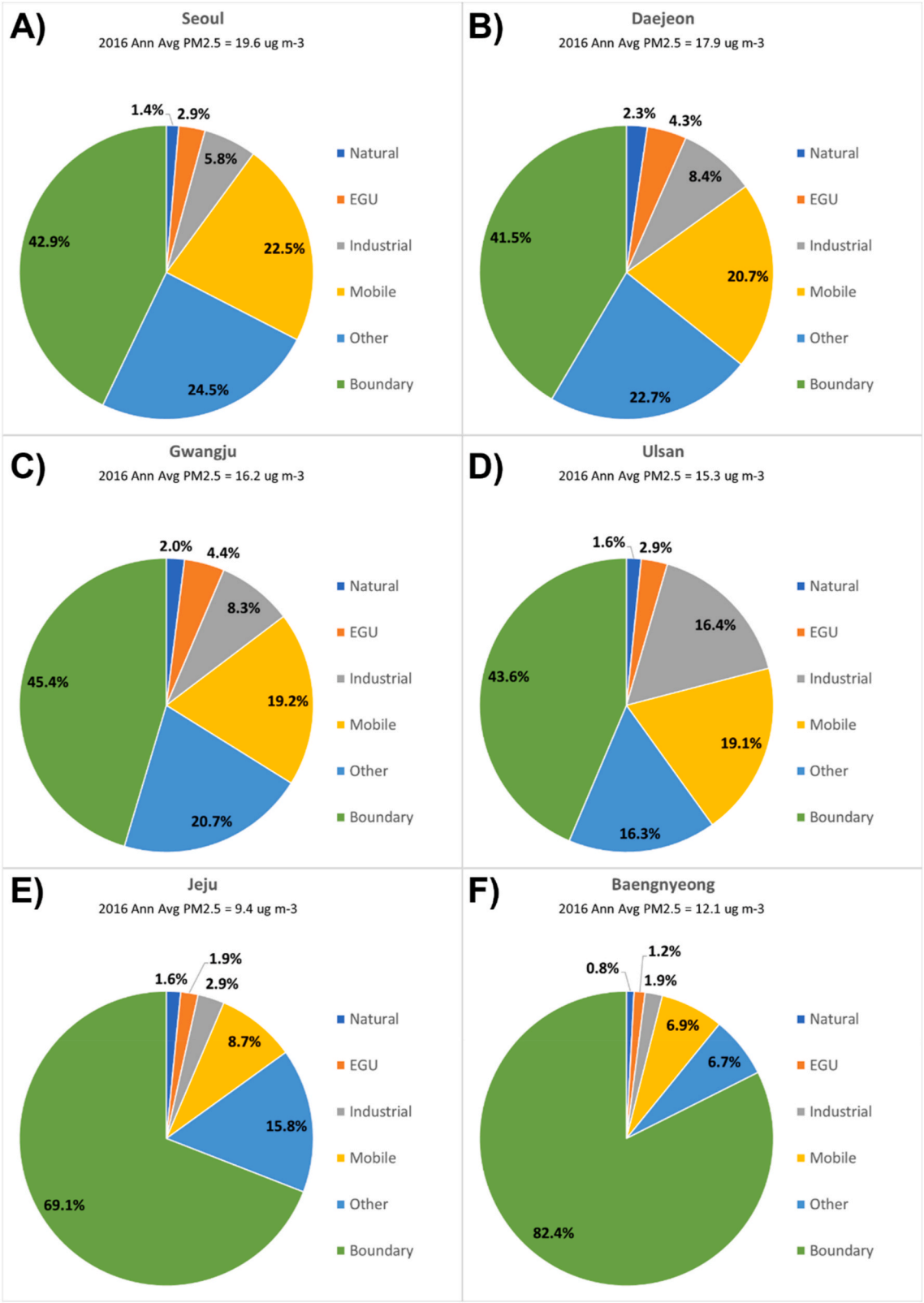

Fig. 12. 2016 annual average PM2.5 contributions by emissions source category for Seoul (top left), Daejeon (top right), Gwangju (middle left), Ulsan (middle right), Jeju (bottom left), and Baengnyeong (bottom right.

8%, and 4%, respectively. For 2015, the contributions were similar for different sources. For example, on an annual basis, the contributions from other, mobile, industrial, and EGUs were 23%, 21%, 5%, and 3%, respectively. On the Top 10 p.m.$_{2.5}$ days in 2015, the contributions from other, mobile, industrial, and EGUs were 20%, 21%, 5%, and 4%, respectively. Focusing on the month of March when the $PM_{2.5}$ concentrations were higher than other months, the contributions from other, mobile, industrial, and EGUs were 21%, 18%, 4%, and 4%, respectively,

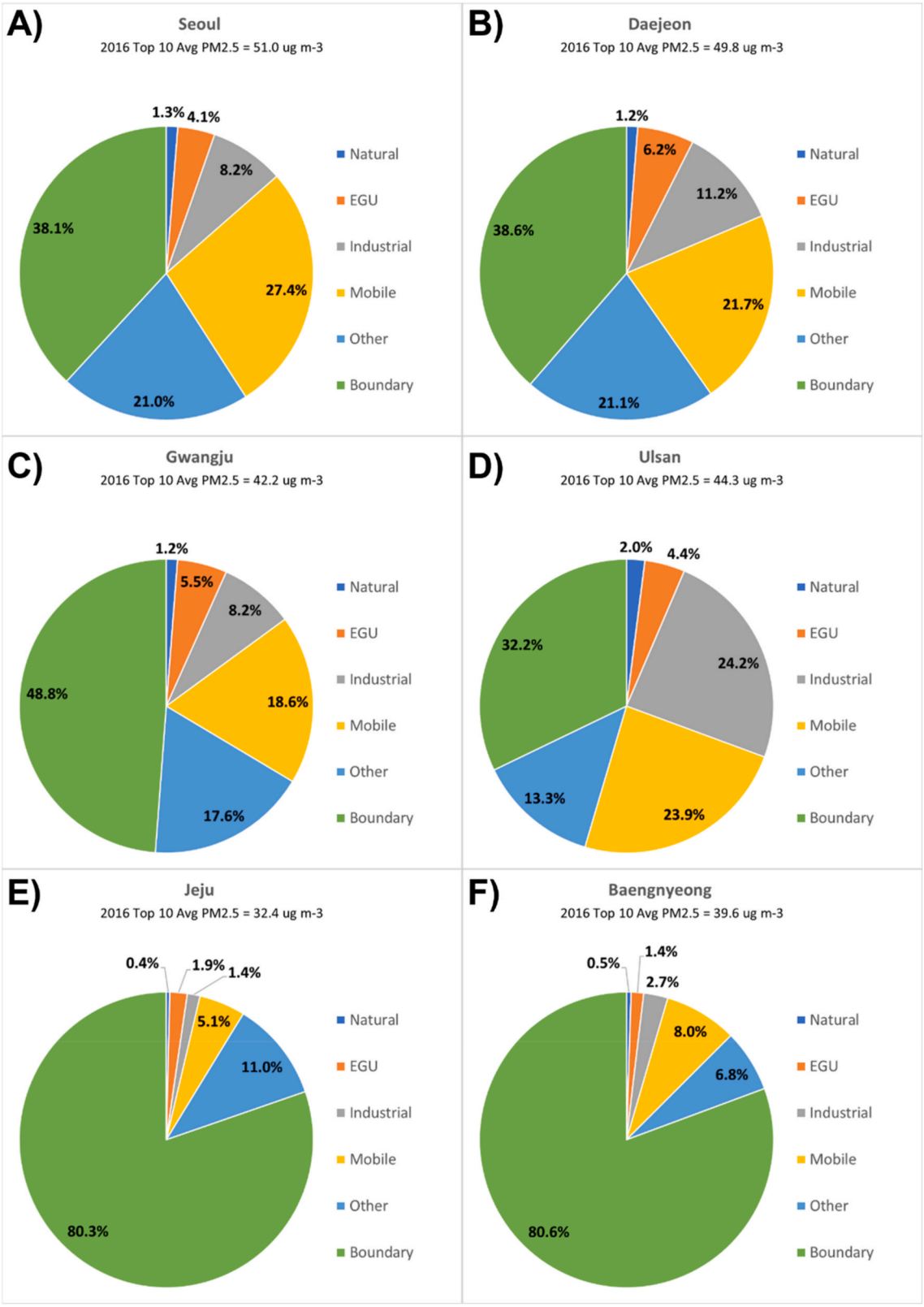

Fig. 13. 2016 annual top 10 p.m.$_{2.5}$ contributions by emissions source category for Seoul (top left), Daejeon (top right), Gwangju (middle left), Ulsan (middle right), Jeju (bottom left), and Baengnyeong (bottom right).

in 2016. For 2015, contributions from these four categories were 18%, 15%, 3%, and 3%, respectively. The percentage contributions from Korean sources are lower in March compared to annual averages because of higher contributions from boundary.

As with any modeling study, this study has some limitations that must be kept in mind when interpreting the results. Our model evaluation analysis showed reasonable model performance for total $PM_{2.5}$; however, there were biases in some of the individual $PM_{2.5}$ components.

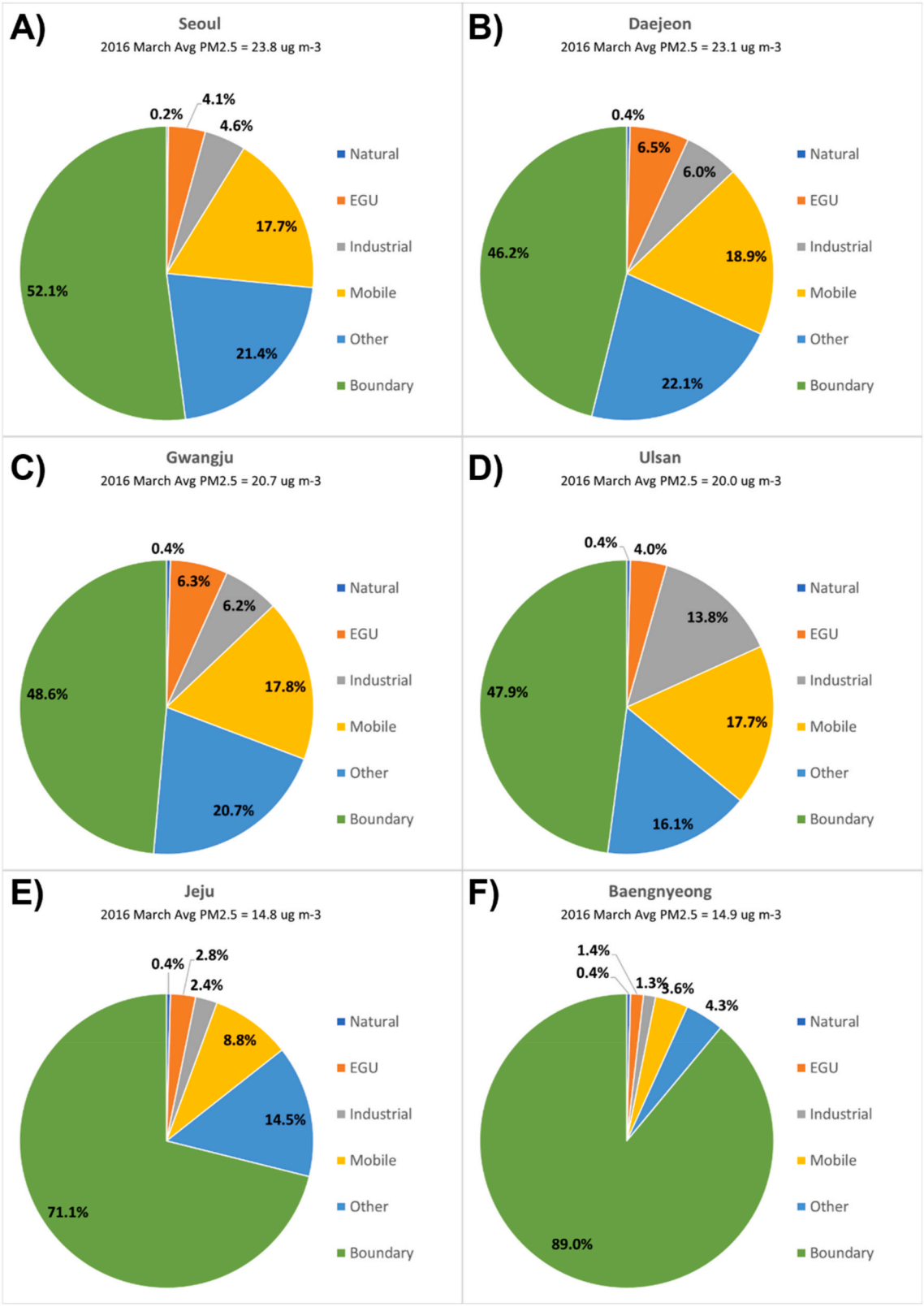

Fig. 14. 2016 March average $PM_{2.5}$ contributions by emissions source category for Seoul (top left), Daejeon (top right), Gwangju (middle left), Ulsan (middle right), Jeju (bottom left), and Baengnyeong (bottom right).

In addition, our evaluation of emissions showed that some limitations exist in Korean emissions estimates. We found large uncertainty in ammonia and biogenic emissions in Korea as well as in windblown and fugitive dust emissions. Any potential errors in emissions can affect the modeling simulations and therefore affect the contribution from sources contributing to organic aerosol (for example, mobile sources) and other components of PM. We investigated contributions from different sources and regions for two different meteorological years to account for the

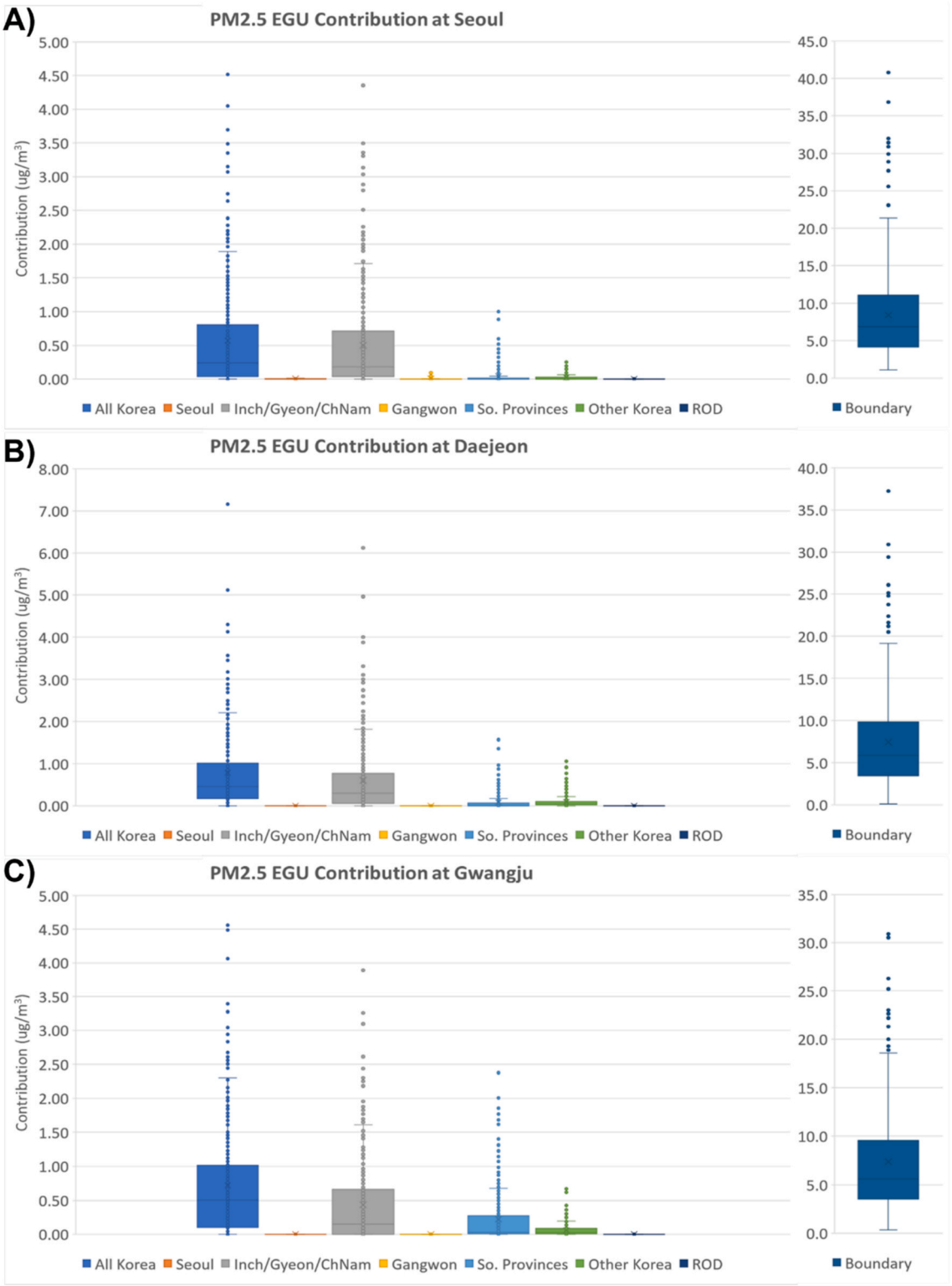

Fig. 15. 2016 24-h average $PM_{2.5}$ EGU contributions by emissions source region at Seoul (top), Daejeon (middle), and Gwangju (bottom). Note that the scale maximum varies. Inc/Gyeon/ChNam refers to Incheon, Gyeonggi, and ChungNam Provinces; So. Provinces refers to Busan, Gyeongnam, Ulsan, and Jeonnam Provinces; ROD refers to Rest of Domain.

variability in meteorology. However, the two years simulated (2015 and 2016) may still not account for the differences in prevailing transport patterns, so contributions from different sources and regions may vary in other years even if emissions do not change.

5. Conclusion

Although there have been previous studies that examined source contributions to PM2.5 within Korea, our study performed a detailed modeling analysis to estimate contributions to $PM_{2.5}$ in Korea from different sources and source regions and for two different years. Our

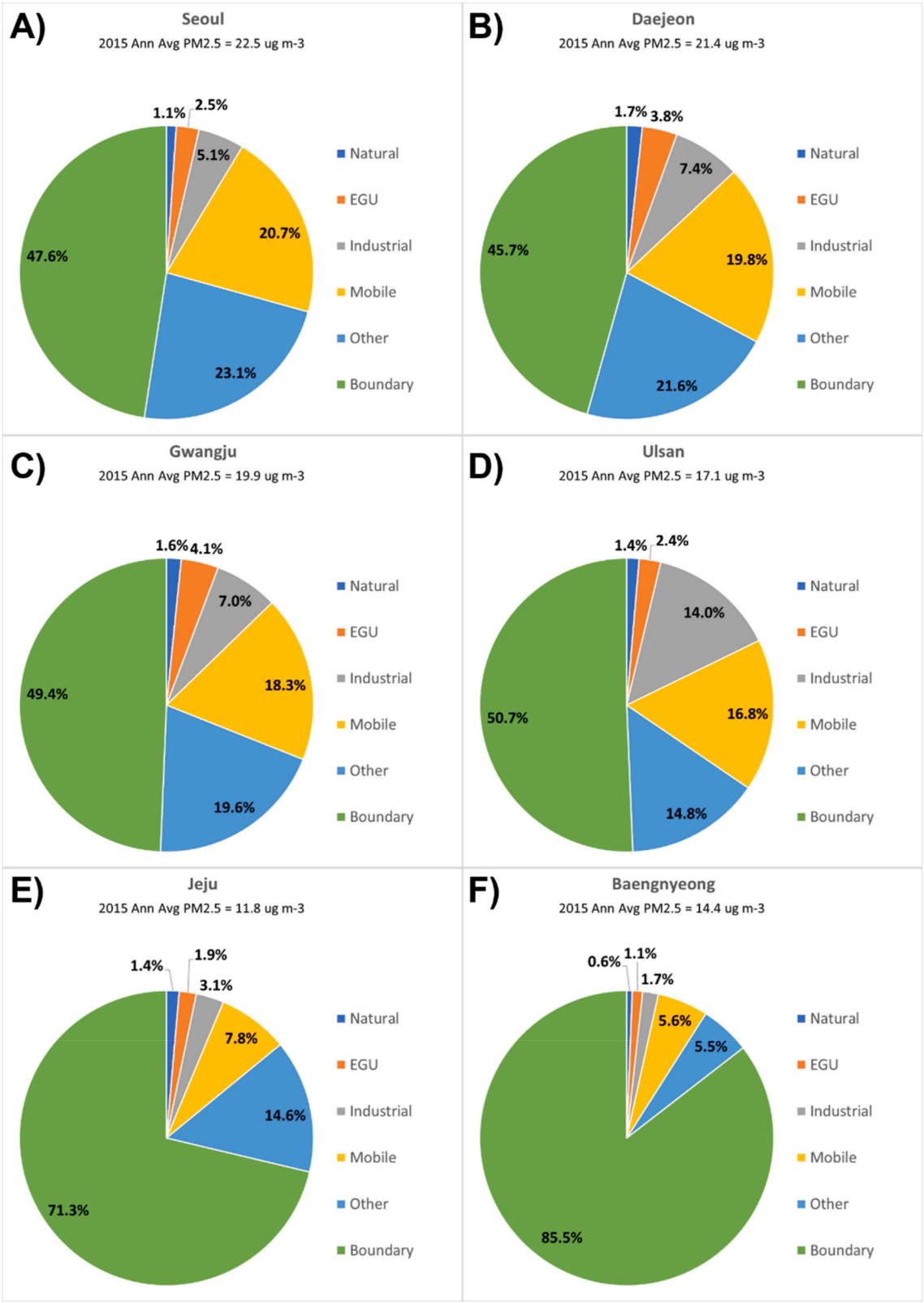

Fig. 16. 2015 annual average $PM_{2.5}$ contributions by emissions source category for Seoul (top left), Daejeon (top right), Gwangju (middle left), Ulsan (middle right), Jeju (bottom left), and Baengnyeong (bottom right).

results are qualitatively similar to previous studies with some important differences. For example, Ryou et al. (2018) found that motor vehicles, soil dust, and combustion/industry sources were the biggest domestic contributors to PM_{10} and $PM_{2.5}$ in the country. Our study also found that mobile sources and industrial sources were among the biggest domestic contributors to PM2.5 in both the years (2015 and 2016). Other receptor modeling studies have shown that secondary aerosols (nitrate, sulfate, organics) and mobile sources to be among the highest domestic

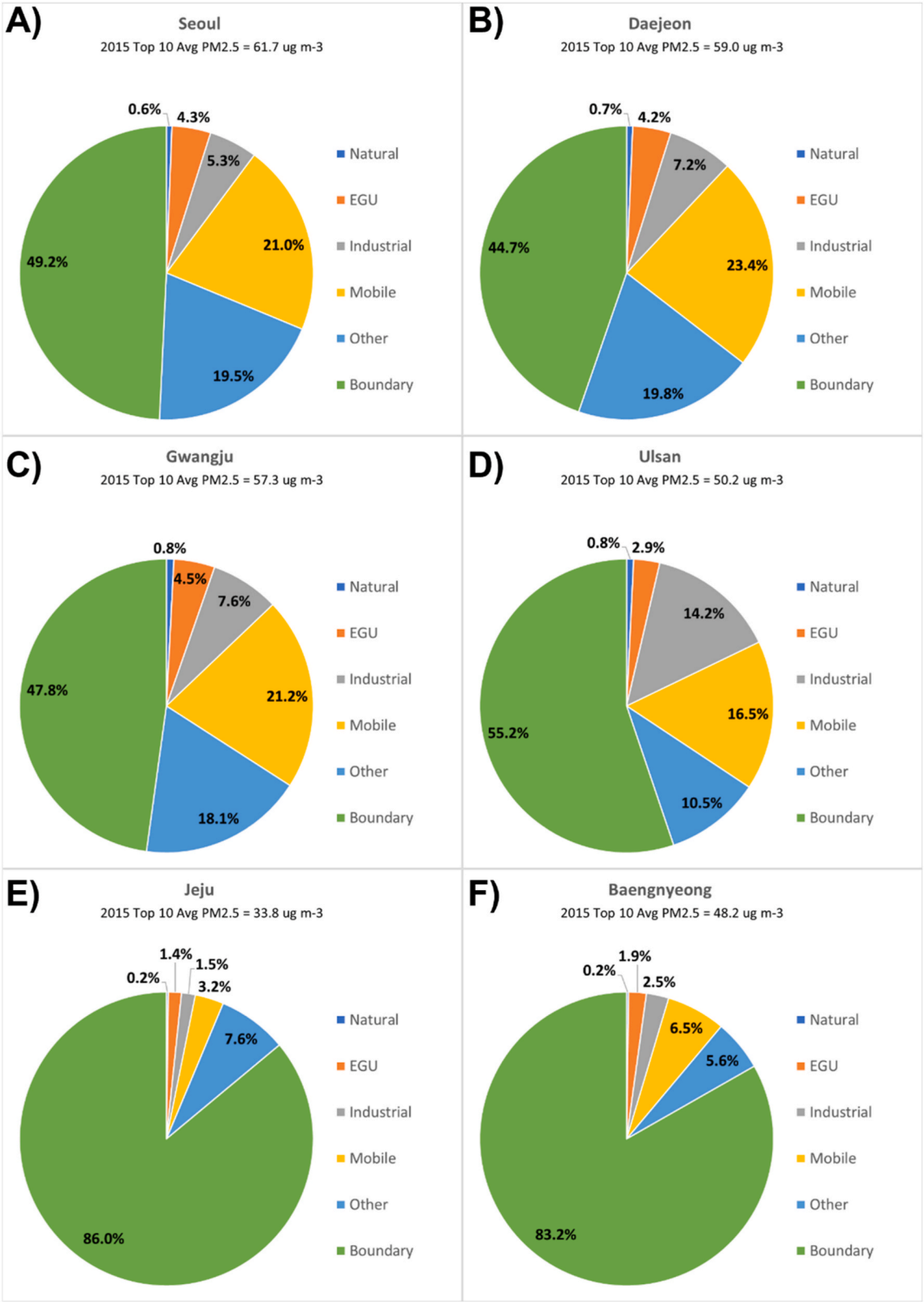

Fig. 17. 2015 annual top 10 $p.m._{2.5}$ contributions by emissions source category for Seoul (top left), Daejeon (top right), Gwangju (middle left), Ulsan (middle right), Jeju (bottom left), and Baengnyeong (bottom right).

contributors to PM2.5 in Korea, which also qualitatively matches our results. Our results also show that "other" emissions sector (includes marine shipping, agricultural ammonia, and international emissions from North Korea and Japan within the CAMx domain) was the highest contributor to PM2.5 in Korea on an annual basis. Given that this sector includes multiple sources, future work could separate these sources further to estimate individual contributions from different sources.

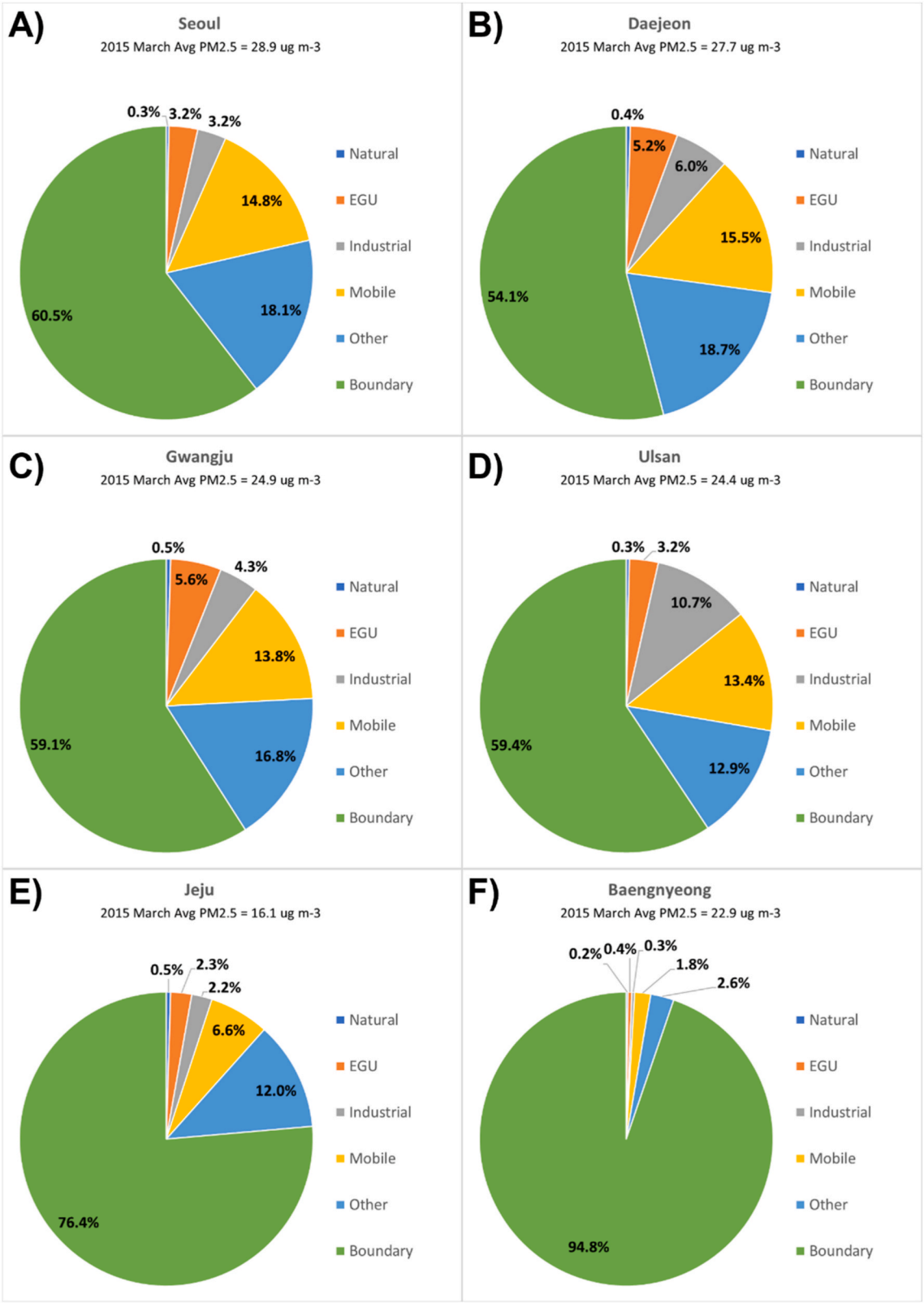

Fig. 18. 2015 March average $PM_{2.5}$ contributions by emissions source category for Seoul (top left), Daejeon (top right), Gwangju (middle left), Ulsan (middle right), Jeju (bottom left), and Baengnyeong (bottom right).

CRediT authorship contribution statement

Naresh Kumar: Conceptualization, Methodology, Writing – original draft, Supervision, Project administration, Funding acquisition. **Jeremiah Johnson:** Methodology, Formal analysis, Investigation, Writing – review & editing, Visualization. **Greg Yarwood:** Methodology, Investigation, Resources, Writing – review & editing, Supervision. **Jung-Hun Woo:** Methodology, Formal analysis, Investigation,

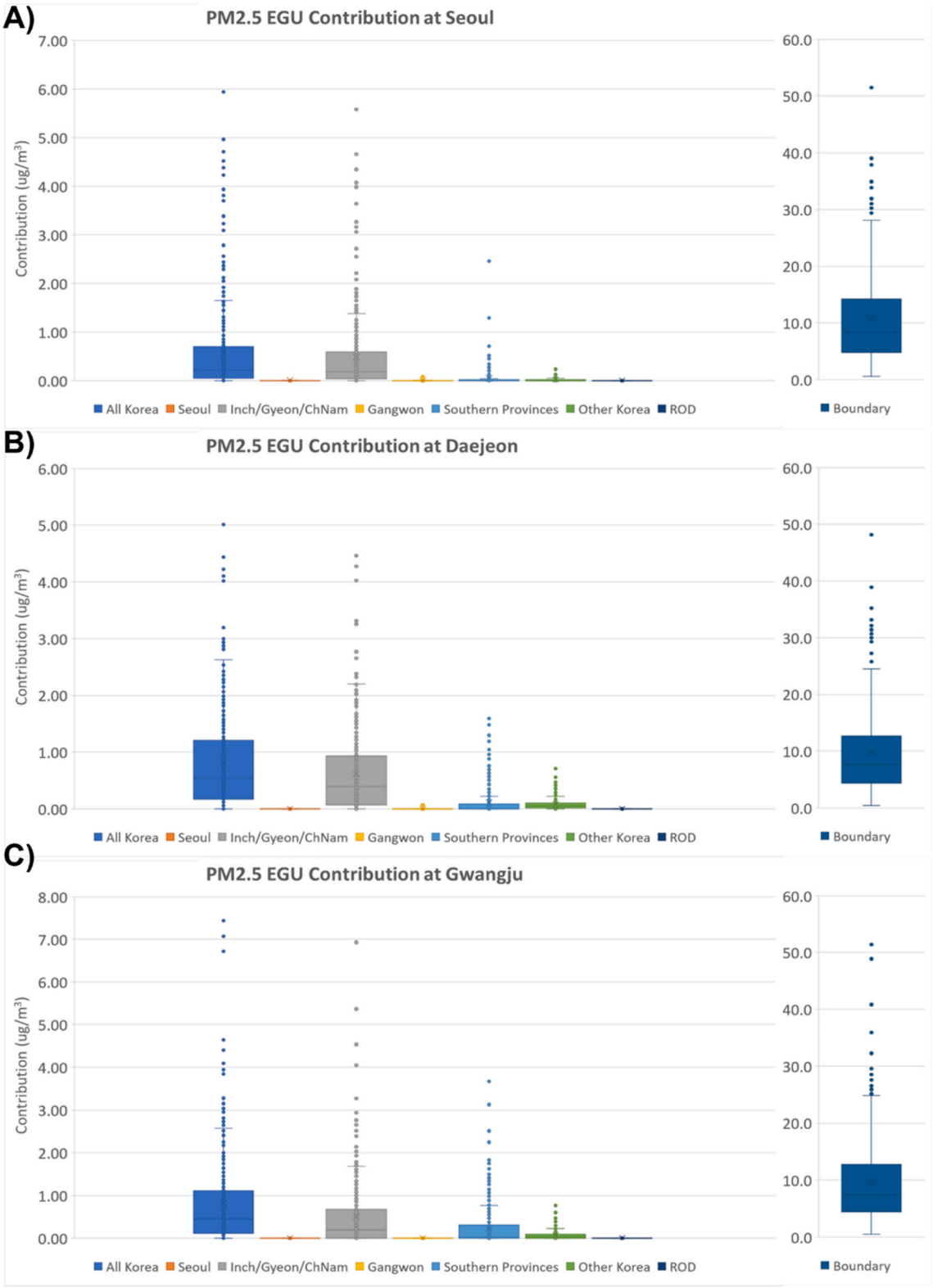

Fig. 19. 2015 24-h average $PM_{2.5}$ EGU contributions by emissions source region at Seoul (top), Daejeon (middle), and Gwangju (bottom). Note that the scale maximum varies. Inc/Gyeon/ChNam refers to Incheon, Gyeonggi, and ChungNam Provinces; So. Provinces refers to Busan, Gyeongnam, Ulsan, and Jeonnam Provinces; ROD refers to Rest of Domain.

Resources, Writing – review & editing, Supervision. **Younha Kim:** Software, Formal analysis, Investigation, Visualization. **Rokjin J. Park:** Methodology, Formal analysis, Investigation, Supervision. **Jaein I. Jeong:** Software, Validation, Formal analysis, Investigation. **Suji Kang:** Conceptualization, Resources, Project administration. **Sungnam Chun:** Conceptualization, Resources, Supervision, Project administration, Funding acquisition. **Eladio Knipping:** Conceptualization, Methodology, Writing – review & editing, Project administration.

Table 7
2015 and 2016 annual average $PM_{2.5}$ contributions by emissions source region at supersites.

Location	Total $PM_{2.5}$		Local [a]				Other Korea				ROD				Boundary			
	2015	2016	2015		2016		2015		2016		2015		2016		2015		2016	
	μg m-3	μg m-3	μg m-3	%	μg m-3	%	μg m-3	%	μg m-3	%	μg m-3	%	μg m-3	%	μg m-3	%	μg m-3	%
Seoul	22.5	19.6	3.4	15	3.3	17	6.8	30	6.6	34	1.5	7	1.4	7	10.7	48	8.4	43
Daejeon	21.4	17.9	5.4	25	5.0	28	5.7	27	5.0	28	0.5	2	0.5	3	9.8	46	7.4	42
Gwangju	19.9	16.2	5.3	27	5.1	31	4.4	22	3.4	21	0.4	2	0.3	2	9.8	49	7.4	45
Ulsan	17.1	15.3	5.0	29	5.1	33	3.2	19	3.3	21	0.2	1	0.2	2	8.7	51	6.7	44
Jeju	11.8	9.4	2.1	18	1.9	20	1.2	10	0.9	10	0.1	1	0.1	1	8.4	71	6.5	69
Baengnyeong	14.4	12.1	0.9	7	0.9	8	0.5	3	0.5	4	0.7	5	0.7	6	12.3	85	10.0	82

[a] The local contribution is from the source region that contains the named location (see Fig. 2 for source regions).

Table 8
2015 and 2016 annual average $PM_{2.5}$ contributions by emissions source category at supersites.

Location	Total		EGU				Industrial				Mobile				Natural + Other			
	2015	2016	2015		2016		2015		2016		2015		2016		2015		2016	
	μg m-3	μg m-3	μg m-3	%	μg m-3	%	μg m-3	%	μg m-3	%	μg m-3	%	μg m-3	%	μg m-3	%	μg m-3	%
Seoul	22.5	19.6	0.6	3	0.6	3	1.1	5	1.1	6	4.7	21	4.4	22	5.4	24	5.1	26
Daejeon	21.4	17.9	0.8	4	0.8	4	1.6	7	1.5	8	4.2	20	3.7	21	5.0	23	4.5	25
Gwangju	19.9	16.2	0.8	4	0.7	4	1.4	7	1.3	8	3.6	18	3.1	19	4.2	21	3.7	23
Ulsan	17.1	15.3	0.4	2	0.4	3	2.4	14	2.5	16	2.9	17	2.9	19	2.8	16	2.7	18
Jeju	11.8	9.4	0.2	2	0.2	2	0.4	3	0.3	3	0.9	8	0.8	9	1.9	16	1.6	17
Baengnyeong	14.4	12.1	0.2	1	0.1	1	0.2	2	0.2	2	0.8	6	0.8	7	0.9	6	0.9	8

Declaration of competing interest

The authors declare that they have no known competing financial interests or personal relationships that could have appeared to influence the work reported in this paper.

Acknowledgements

This publication was made possible by funding from the Electric Power Research Institute (EPRI). Rokjin J. Park and Jaein I. Jeong were also supported by Korea Environment Industry & Technology Institute (KEITI) through Public Technology Program based on Environmental Policy Program, funded by Korea Ministry of Environment (MOE) (2019000160002). Publication's contents are solely the responsibility of the grantee and do not necessarily represent the official views of the supporting agencies.

Appendix A. Supplementary data

Supplementary data to this article can be found online at https://doi.org/10.1016/j.atmosenv.2022.119273.

References

ENVIRON, Alpine, 2012. Western Regional Air Partnership (WRAP) West-wide Jump-Start Air Quality Modeling Study (WestJump AQMS) – WRF Application/Evaluation. ENVIRON International Corporation, Novato, California. Alpine Geophysics, LLC. University of North Carolina. February 29. https://www.wrapair2.org/pdf/WestJumpAQMS_2008_Annual_WRF_Final_Report_February29_2012.pdf.

NIER and NASA, 2017. KORUS-AQ Rapid Science Synthesis Report.

Bae, C., Kim, B.-U., Kim, H.C., Yoo, C., Kim, S., 2019. Long-range transport influence on key chemical components of PM2.5 in the Seoul metropolitan area, South Korea, during the years 2012–2016. Atmosphere. https://doi.org/10.3390/atmos11010048. IF 2.397.

Bae, M., Kim, B.-U., Kim, H.C., Kim, S., 2020. A Multiscale tiered approach to quantify contributions: a case study of $PM_{2.5}$ in South Korea during 2010–2017. Atmosphere 11, 141, 2020.

Choi, J.K., Heo, Jong-Bae, Ban, Soo-Jin, Yi, Seung-Muk, Zoh, Kyung-Duk, 2013. Source apportionment of PM2.5 at the coastal area in Korea. Sci. Total Environ. 447, 370–380. https://doi.org/10.1016/j.scitotenv.2012.12.047. ISSN 0048-9697.

Choi, J., Park, R.J., Lee, H.-M., Lee, S., Jo, D.S., Jeong, J.I., Henze, D.K., Woo, J.-H., Ban, S.-J., Lee, M.-D., Lim, C.-S., Park, M.-K., Shin, H.J., Cho, S., Peterson, D., Song, C.-K., 2019. Impacts of Local vs. Trans-boundary Emissions from Different Sectors on PM2.5 Exposure in South Korea during the KORUS-AQ Campaign. https://doi.org/10.1016/j.atmosenv.2019.02.008.

CMAS, 2018. SMOKE modeling System. available at: https://www.cmascenter.org/smoke/. (Accessed 5 December 2018).

Emery, C., Tai, E., Yarwood, G., 2001. Enhanced Meteorological Modeling and Performance Evaluation for Two Texas Ozone Episodes. Prepared for the Texas Natural Resource Conservation Commission prepared by ENVIRON.

Emery, C., Koo, B., Hsieh, W.-C., Wentland, A., Wilson, G., Yarwood, G., 2016. Updated Carbon Bond Chemical Mechanism. Technical Memorandum prepared for US Environmental Protection Agency, Novato, CA. EPA Contract EPD12044. Ramboll.

Emery, C., Liu, Z., Russell, A.G., Odman, M.T., Yarwood, G., Kumar, N., 2017. Recommendations on statistics and benchmarks to assess photochemical model performance. J. Air Waste Manag. Assoc. 67 (5), 582–598. https://doi.org/10.1080/10962247.2016.1265027.

Friedl, M.A., Sulla-Menashe, D., Tan, B., Schneider, A., Ramankutty, N., Sibley, A., Huang, X., 2010. MODIS Collection 5 global land cover: algorithm refinements and characterization of new data sets. Remote Sens. Environ. 114, 168–182. https://doi.org/10.1016/j.rse.2009.08.016.

Gong, S.L., 2003. A parameterization for sea-salt aerosol source function for sub- and super-micron particle sizes. Biogeochemical Cycles 17, 1097–1104.

Harvard University, 2018. The GEOS-Chem Model Web Page. Available at: http://acmg.seas.harvard.edu/geos/index.html. June 4, 2019).

Heo, J.-B., Hopke, P.K., Yi, S.-M., 2009. Source apportionment of $PM_{2.5}$ in Seoul, Korea. Atmos. Chem. Phys. 9, 4957–4971. https://doi.org/10.5194/acp-9-4957-2009.

Jeong, J.-H., Shon, Zang-Ho, Kang, Minsung, Song, Sang-Keun, Kim, Yoo-Keun, Park, Jinsoo, Kim, Hyunjae, 2017. Comparison of source apportionment of PM2.5 using receptor models in the main hub port city of East Asia: Busan. Atmos. Environ. 148, 115–127. https://doi.org/10.1016/j.atmosenv.2016.10.055. ISSN 1352-2310.

Kim, Y.P., Lee, G., 2018. Trend of air quality in Seoul: policy and science. Aerosol Air Qual. Res. 18, 2141–2156. https://doi.org/10.4209/aaqr.2018.03.0081.

Kim, H.C., Kim, E., Bae, C., Cho, J.H., Kim, B.-U., Kim, S., 2017. Regional contributions to particulate matter concentration in the Seoul metropolitan area, South Korea: seasonal variation and sensitivity to meteorology and emissions inventory. Atmos. Chem. Phys. 17, 10315–10332. https://doi.org/10.5194/acp-17-10315-2017.

Kim, Yumi, Seo, Jihoon, Kim, Jin, Young, Lee, Ji, Kim, Hwajin, Kim, Bong, 2018. Characterization of PM2.5 and identification of transported secondary and biomass burning contribution in Seoul, Korea. Environ. Sci. Pollut. Control Ser. 25 https://doi.org/10.1007/s11356-017-0772-x.

Kim, D., Choi, H.E., Gal, W.M., Seo, S., 2020. Five year trends of particulate matter concentrations in Korean regions (2015-2019): when to ventilate? Int. J. Environ. Res. Publ. Health 17 (16), 5764. https://doi.org/10.3390/ijerph17165764. Published 2020 Aug 10.

Korea Ministry of Environment, 2018. Annual Report of Air Quality in Korea 2017. National Institute of Environmental Research, Incheon, South Korea.

Kumar, N., Rokjin, J. Park, Jeong, Jaein I., Woo, Jung-Hun, Kim, Younha, Johnson, Jeremiah, Yarwood, Greg, Kang, Suji, Chun, Sungnam, Knipping, Eladio, 2021. Contributions of International Sources to PM2.5 in South Korea. Atmospheric Environment. https://doi.org/10.1016/j.atmosenv.2021.118542.

Luecken, D.J., Yarwood, G., Hutzell, W.T., 2019. Multipollutant Modeling of Ozone, Reactive Nitrogen and HAPs across the Continental US with CMAQ-CB6, vol. 201. Atmospheric Environment, pp. 62–72.

Mavko, M., Morris, R., 2013. DEASCO3 Project Updates to the Fire Plume Rise Methodology to Model Smoke Dispersion. Technical Memo prepared as part of Join Science Fire Program (JSP) project Deterministic and Empirical Assessment of Smoke's Contribution to Ozone. December 3. https://wraptools.org/pdf/DEASCO3_Plume_Rise_Memo_20131210.pdf.

McNally, D.E., 2009. 12km MM5 Performance Goals." Presentation to the Ad-Hoc Meteorology Group. 25 June. http://www.epa.gov/scram001/adhoc/mcnally2009.pdf.

NCAR, 2018. The weather Research and forecasting model web page. Available at: https://www.mmm.ucar.edu/weather-research-and-forecasting-model. (Accessed 5 December 2018).

Oh, M.-S., Park, C.K., 2020. Regional source apportionment of PM2.5 in Seoul using Bayesian multivariate receptor model. J. Appl. Stat. https://doi.org/10.1080/02664763.2020.1822305.

Ovadnevaite, J., Manders, A., de Leeuw, G., Ceburnis, D., Monahan, C., Partanen, A.-I., Korhonen, H., O'Dowd, C.D., 2014. A sea spray aerosol flux parameterization encapsulating wave state. Atmos. Chem. Phys. 14, 1837–1852. https://doi.org/10.5194/acp-14-1837-2014.

Ramboll, 2019. User's Guide to the Comprehensive Air Quality Model with Extensions. Available at:, version 6.5. www.camx.com. February 5, 2019.

Ryou, H.G., Heo, J., Kim, S.Y., 2018. Source apportionment of PM_{10} and $PM_{2.5}$ air pollution, and possible impacts of study characteristics in South Korea. Sep Environ. Pollut. 240, 963–972. https://doi.org/10.1016/j.envpol.2018.03.066. Epub 2018 Jun 15. Erratum in: Environ Pollut. 2018 Nov;242(Pt B):2135. PMID: 29910064.

Sakulyanontvittaya, T., Duhl, T., Wiedinmyer, C., Helmig, D., Matsunaga, S., Potosnak, M., Milford, J., Guenther, A., 2008. Monoterpene and sesquiterpene emission estimates for the United States. Environ. Sci. Technol. 42, 1623–1629.

Simpson, I.J., Blake, D.R., Blake, N.J., Meinardi, S., Barletta, B., Hughes, S.C., Fleming, L. T., Crawford, J.H., Diskin, G.S., Emmons, L.K., Fried, A., Guo, H., Peterson, D.A., Wisthaler, A., Woo, J.-H., Barré, J., Gaubert, B., Kim, J., Kim, M.J., Kim, Y., Knote, C., Mikoviny, T., Pusede, S.E., Schroeder, J.R., Wang, Y., Wennberg, P.O., Zeng, L., 2020. Characterization, sources and reactivity of volatile organic compounds (VOCs) in Seoul and surrounding regions during KORUS-AQ. Elementa: Science of the Anthropocene 1, 8 37. https://doi.org/10.1525/elementa.434. January 2020.

Son, J.Y., Lee, J.T., Kim, K.H., Jung, K., Bell, M.L., 2012. Characterization of fine particulate matter and associations between particulate chemical constituents and mortality in Seoul, Korea. Environ. Health Perspect. 120 (6), 872–878. https://doi.org/10.1289/ehp.1104316.

US EPA, Air Emission Inventories. Available at: https://www.epa.gov/air-emissions-inventories (accessed November 30, 2018).

Wiedinmyer, C., Friedli, H., 2007. Mercury emission estimates from fires: an initial inventory for the United States. Environ. Sci. Technol. 41 (23), 8092–8098. https://doi.org/10.1021/es071289o, 2007.

Wiedinmyer, C., Quayle, B., Geron, C., Belote, A., McKenzie, D., Zhang, X., O'Neill, S., Klos Wynne, K., 2006. Estimating emissions from fires in North America for air quality modeling. Atmos. Environ. 40 (19), 3419–3432.

Sullivan, J.T., McGee, T.J., Stauffer, R.M., Thompson, A.M., Weinheimer, A., Knote, C., Janz, S., Wisthaler, A., Long, R., Szykman, J., Park, J., Lee, Y., Kim, S., Jeong, D., Sanchez, D., Twigg, L., Sumnicht, G., Knepp, T., Schroeder, J.R., 2019. Taehwa Research Forest: a receptor site for severe domestic pollution events in Korea during 2016. Atmos. Chem. Phys. 19, 5051–5067. https://doi.org/10.5194/acp-19-5051-2019.

Wiedinmyer, C., Akagi, S.K., Yokelson, R.J., Emmons, L.K., Al-Saadi, J.A., Orlando, J.J., Soja, A.J., 2011. The fire inventory from NCAR (Finn): a high-resolution global model to estimate the emissions from open burning. Geosci. Model Dev. (GMD) 4 (3), 625–641. http://www.geosci-model-dev.net/4/625/2011/gmd-4-625-2011.html.

Yarwood, G., Morris, R.E., Wilson, G.M., 2007. Particulate matter source apportionment technology (PSAT) in the CAMx photochemical grid model. Air Pollution Modeling and Its Application XVII 478–492. Springer, Boston, MA.